forests

Article

Colletotrichum Species Causing *Cyclocarya paliurus* Anthracnose in Southern China

Xiang-Rong Zheng [1,2,†], Mao-Jiao Zhang [1,†] and Feng-Mao Chen [1,*]

[1] Collaborative Innovation Center of Sustainable Forestry in Southern China, College of Forestry, Nanjing Forestry University, Nanjing 210037, China; zhengxr@jsafc.edu.cn (X.-R.Z.); zhangmaojiao@njfu.edu.cn (M.-J.Z.)
[2] College of Landscape Architecture, Jiangsu Vocational College of Agriculture and Forestry, Zhenjiang 212400, China
* Correspondence: cfengmao@njfu.edu.cn
† These authors contributed equally to this work.

Abstract: *Cyclocarya paliurus*, native to China, is a medicinal and edible plant with important health benefits. Anthracnose is an emerging disease in southern China that causes severe economic losses and poses a great threat to the *C. paliurus* tea industry. However, to date, the species diversity of pathogens causing *C. paliurus* anthracnose has remained limited. From 2018 to 2022, a total of 331 *Colletotrichum* isolates were recovered from symptomatic leaves in eight major *C. paliurus* planting provinces of southern China. Phylogenetic analyses based on nine loci (ITS, *GAPDH*, *ACT*, *CHS-1*, *TUB*, *CAL*, *HIS3*, *GS* and *ApMat*) coupled with phenotypic characteristics revealed that 43 representative isolates belonged to seven known *Colletotrichum* species, including *C. brevisporum*, *C. fructicola*, *C. gloeosporioides* sensu stricto, *C. godetiae*, *C. nymphaeae*, *C. plurivorum* and *C. sojae*. Pathogenicity tests demonstrated that all species described above were pathogenic to wounding detached leaves of *C. paliurus*, with *C. fructicola* being the most aggressive species. However, *C. brevisporum*, *C. plurivorum* and *C. sojae* were not pathogenic to the intact plant of *C. paliurus*. These findings reveal the remarkable species diversity involved in *C. paliurus* anthracnose and will facilitate further studies on implementing effective control of *C. paliurus* anthracnose in China.

Keywords: *Cyclocarya paliurus* anthracnose; *Colletotrichum*; prevalence; species diversity; polyphasic approach

Citation: Zheng, X.-R.; Zhang, M.-J.; Chen, F.-M. *Colletotrichum* Species Causing *Cyclocarya paliurus* Anthracnose in Southern China. *Forests* **2024**, *15*, 490. https://doi.org/10.3390/f15030490

Academic Editors: Young-Seuk Park and Jun-Jun Liu

Received: 31 January 2024
Revised: 28 February 2024
Accepted: 4 March 2024
Published: 6 March 2024

1. Introduction

Cyclocarya paliurus (Batal.) Iljinsk., commonly called "sweet tea" in China, is the sole extant species belonging to the Juglandaceae family, and is naturally distributed in the central southern mountains [1]. In Chinese folk medicine, leaves of *C. paliurus* have been used in traditional tea or medicine for the treatment of diabetes mellitus or obesity for more than 1000 years [2]. In recent years, considerable attention has been given to *C. paliurus* because pharmacological studies have suggested that its leaves exhibit hypoglycaemic [3], hypolipidemic [4], antioxidant [5], anti-HIV-1 [6] and anticancer [7] properties. Consequently, *C. paliurus* leaves were investigated as a substitute for common tea (*Camellia sinensis*) and authorized as a new food raw material by the National Health and Family Planning Commission of China in 2013 [8]. During the past few years, large-scale plantings of *C. paliurus* have been established for leaf-harvesting to meet the increasing demand for tender *C. paliurus* leaves for tea production or medical use in China [9]. The cultivation of *C. paliurus* is beneficial for the national economy and livelihoods of local farmers but also leads to infectious diseases.

The destructive pathogens causing *C. paliurus* anthracnose were attributed exclusively to *Colletotrichum* spp. within the *C. gloeosporioides* species complex [10], which are also responsible for anthracnose on numerous tree species and crops in subtropical and tropical regions. Although historical data are unavailable, it has been recently reported in Jiangsu

Province that the incidence of *C. paliurus* anthracnose can reach 64% in some newly established plantations and can also result in mortality of branches and even plants in severe cases [10]. In the presence of appropriate temperatures and high moisture conditions in the fields of southern China, *Colletotrichum* spp. can form fruiting bodies and spread rapidly; thus, anthracnose leads to significant losses in yield and economy, ultimately posing a major threat to the *C. paliurus* tea industry in China [11].

C. paliurus anthracnose is considered an emerging and serious disease since multiple *Colletotrichum* species can coexist on a single host plant, even within the same lesion [10]. Hence, accurate identification of the *Colletotrichum* spp. associated with *C. paliurus* anthracnose is highly important for understanding its epidemiology and effective application of management strategies. Identification and circumscription of *Colletotrichum* spp. have historically been based on symptoms in particular hosts, host range and a series of morphological features [12]. Nevertheless, the use of these conventional criteria has failed to delimit *Colletotrichum* spp. due to phenotypic variations in the same species under different environmental conditions [12,13]. According to Liu et al. [14], the current classification system of *Colletotrichum* comprises 15 species complexes, all of which can be differentiated from each other by utilizing the internal transcribed spacer (ITS) region alone, whereas the species-within-species complex can be resolved by sequence differences in additional genes, such as five loci (*GADPH*, *CHS-1*, *HIS3*, *ACT* and *TUB*) that have been used for the *C. acutatum* (Acutatum) and *C. orchidearum* (Orchidearum) species complexes [15,16], while two additional loci (GS and ApMat) have been employed for the *C. gloeosporioides* (Gloeosporioides) species complex [13,17].

Anthracnose has increasingly aroused concern among growers in the *C. paliurus* tea-producing areas of southern China. Hence, the objectives of this study were (i) to investigate the diversity of *Colletotrichum* species associated with *C. paliurus* anthracnose among the major production provinces in southern China based on morphological features and phylogenetic analyses and (ii) to determine the distribution and pathogenicity of these *Colletotrichum* species in the region.

2. Materials and Methods

2.1. Sample Collection and Fungal Isolation

From July to October in 2018–2022, *C. paliurus* leaves exhibiting typical anthracnose symptoms (Figure 1) were collected from the eight main *C. paliurus* tea-producing provinces (Fujian, Guangxi, Guizhou, Hubei, Hunan, Jiangxi, Sichuan, and Zhejiang; Table A3) of southern China. One commercial plantation was surveyed per location/county. Before sampling, the disease incidence was estimated by randomly counting and rating 100 plants after zigzag walking throughout the orchards. In total, 83 leaf samples were obtained (Table A3). Symptomatic leaves were examined with a ZEISS Stereo Microscope (Discovery V20, Carl Zeiss, Oberkochen, Germany) to observe asexual or sexual fungal structures for preliminary identification. Foliar fragments (lesion margin; 4 mm in side length) without sporulation were surface-sterilized (1% NaClO for 45 s, followed by 70% ethanol for 45 s, rinsed in sterile distilled water three times and dried), placed to potato dextrose agar (PDA; 200 g/L of potato; 20 g/L of glucose; 20 g/L of agar; Solarbio, Beijing, China) plates supplemented with 100 μg/mL ampicillin, and incubated at 25 °C in the dark. For symptomatic leaves with sporulation, conidial suspensions were collected by rinsing fruiting bodies with sterile distilled water, diluted to a concentration of 1×10^4 cfu/mL, and coating them on the surface of 2% water agar (WA; Solarbio, China) [18]. The edges of the emerging myceliawere were transferred onto fresh PDA plates, and pure cultures were obtained by single spore (conidium or ascospore) isolation following the methods of Cai et al. [19]. Representative isolates were deposited at Nanjing Forestry University (NJFU) and the Microbiological Culture Collection Centre at Jiangsu Vocational College of Agriculture and Forestry (JSAFC).

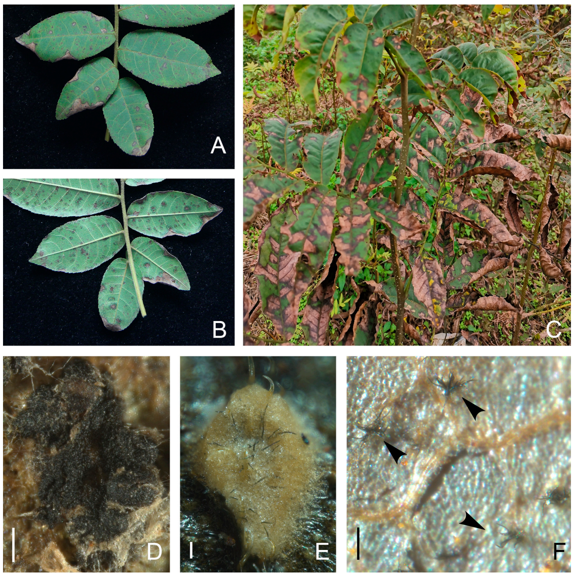

Figure 1. Typical symptoms of *Cyclocarya paliurus* anthracnose. (**A**) Front and (**B**) reverse view of irregular necrotic lesions on leaves; (**C**) field symptoms; (**D**) *Colletotrichum* fruiting bodies of ascomata and (**E**,**F**) Acervuli developed on diseased leaf tissues, with arrows point to setae. Scale bars: (**D**) =200 µm; (**E**) =50 µm; (**F**) =100 µm.

2.2. Molecular Identification

2.2.1. DNA Extraction

Aerial mycelia of each single-spore isolate were collected with a sterile scalpel from a 5-day-old colony and placed in a sterile 2 mL centrifuge tube. Total genomic DNA was extracted using a Genomic DNA Extraction Kit (D2300, Solarbio, Beijing, China) following the manufacturer's instructions. DNA concentrations were quantified using a Nanodrop 2000 spectrophotometer (Thermo Scientific, Waltham, MA, USA), and the DNA was manually diluted to 100 ng/µL for polymerase chain reaction (PCR) amplification.

2.2.2. Multigene Amplification and Sequencing

As an initial analysis of genetic diversity, portions of the ITS and *GADPH* loci were amplified from all the isolates to select representative sequences for further multilocus phylogenetic analysis The genetic loci and primers used for amplification and sequencing are listed in Table 1.

Table 1. Genetic loci and primers used in this study.

Loci	Product Name	Primer	Direction	Sequence (5′-3′)	Reference
ITS	Internal transcribed spacer	ITS1F	Forward	CTTGGTCATTTAGAGGAAGTAA	Gardes and Bruns [20]
		ITS4	Reverse	TCCTCCGCTTATTGATATGC	White et al. [21]
GAPDH	Glyceraldehyde-3-phosphate dehydrogenase	GDF1	Forward	GCCGTCAACGACCCCTTCATTGA	Guerber et al. [22]
		GDR1	Reverse	GGGTGGAGTCGTACTTGAGCATGT	Guerber et al. [22]
CHS-1	Chitin synthase 1	CHS-79F	Forward	TGGGGCAAGGATGCTTGGAAGAAG	Carbone and Kohn [23]
		CHS-354R	Reverse	TGGAAGAACCATCTGTGAGAGTTG	Carbone and Kohn [23]
HIS3	histone H3	CYLH3F	Forward	AGGTCCACTGGTGGCAAG	Crous et al. [24]
		CYLH3R	Reverse	AGCTGGATGTCCTTGGACTG	Crous et al. [24]
ACT	Actin	ACT-512F	Forward	ATGTGCAAGGCCGGTTTCGC	Carbone and Kohn [23]
		ACT-783R	Reverse	TACGAGTCCTTCTGGCCCAT	Carbone and Kohn [23]
TUB	β-tubulin	T1	Forward	AACATGCGTGAGATTGTAAGT	O'Donnell and Cigelnik [25]
		Bt-2b	Reverse	ACCCTCAGTGTAGTGACCCTTGGC	Glass and Donaldson [26]
CAL	Calmodulin	CL1A	Forward	GATCAAGGAGGCCTTCTC	O'Donnell et al. [27]
		CL2A	Reverse	TTTTTGCATCATGAGTTGGAC	O'Donnell et al. [27]
GS	Glutamine synthetase	GSLF2	Forward	TACACGAGSAAAAGGATACGC	Liu et al. [17]
		GSLR1	Reverse	AGRCGCACATTGTCAGTATCG	Liu et al. [17]
ApMat	Apn2-Mat1-2 intergenic spacer	AM-F	Forward	TCATTCTACGTATGTGCCCG	Silva et al. [28]
		AM-R	Reverse	CCAGAAATACACCGAACTTGC	Silva et al. [28]

The procedure and conditions for PCR amplification were adopted from Zheng et al. [10], except for *HIS3*, for which the annealing temperature was 55 °C. The amplification products were visualized on a 1.2% agarose gel after electrophoresis (120 V, 20 min), and positive amplicons were purified and sequenced by Sangon Biotechnology Company (Shanghai, China). The forward and reverse sequences of all representative isolates were assembled, and consensus sequences were deposited in GenBank (Tables A1 and A2).

2.2.3. Phylogenetic Analyses

Reference sequences from authentic specimens of the Gloeosporioides, Acutatum, Magnum and Orchidearum complexes were retrieved from GenBank and aligned with sequences generated in the present study to construct phylogenetic trees. *Monilochaetes infuscans* (CBS 869.96) was included as the outgroup taxon. Sequence alignments of each locus were performed with BioEdit (version 7.1.9) and optimized by manual adjustment to allow for maximum alignment. Subsequently, multiple loci were concatenated with SequenceMatrix 1.8 [29].

The concatenated sequences of different gene combinations were used to infer phylogenetic relationships under the maximum-likelihood (ML) and Bayesian inference (BI) criteria, implemented in MEGA X [30] and MrBayes 3.2.6 [31], respectively. MEGA was first used to determine the best model of nucleotide substitution for the combined dataset using the Akaike Information Criterion (AIC). The ML analysis utilized the nearest-neighbor-interchange (NNI) heuristic search method, with clade stability assessed by 1000 bootstrap replicates [30]. For BI, two independent analyses were conducted with four Markov chains, evaluating 3×10^6 generations, with samples taken every 1000th generation. Posterior probabilities (PPs) were calculated after discarding the first 25% of generations as burn-in. A PP equal to 1.00 and bootstrap values (Bv) greater than 85% were taken as evidence for branch support. The consensus tree was visualized using FigTree (version 1.3.1).

2.3. Phenotypic Analysis

For macroscopic and microscopic characterization of representative *Colletotrichum* isolates, mycelial blocks (2–3 mm^2) were aseptically removed from the edge of actively growing cultures, transferred to fresh PDA and synthetic nutrient-poor agar (SNA [18]) plates and incubated as described above. The culture characteristics were recorded at 6 days after inoculation, and images of the upper and lower surfaces of the colonies were taken. The colony diameters on the PDA plates were measured at 24 h intervals to calculate the mean daily growth (mm/d). The experiment was performed as a randomized complete block, with three replicates for each isolate. Conidial and ascospore suspensions of each selected isolate were prepared in sterile water from conidial masses and ascomata on PDA plates, respectively. Conidial appressoria were induced via a previously published technique [32]. The conidiophores were observed on the colonies grown on PDA or SNA plates. At least 100 measurements were conducted for each *Colletotrichum* fungal structure (conidia, appressoria and ascospores) with a ZEISS fluorescence microscope (Axio Imager A2m, Carl Zeiss, Germany) using differential interference contrast.

2.4. Pathogenicity Tests

Three representative isolates of each identified *Colletotrichum* species were selected to confirm their pathogenicity on detached leaves and whole plants of *C. paliurus* using the mycelial plug method because some *Colletotrichum* species showed no satisfactory sporulation on culture media. Prior to inoculation, asymptomatic leaves of *C. paliurus* were surface-disinfected and air-dried as described above.

To inoculate the detached *C. paliurus* leaves, both wounding and nonwounding techniques were utilized. A mycelial plug (5 mm in diameter) was prepared from a fresh colony as mentioned above, and the plug was adhered to the adaxial surface of each leaf, which was punctured with a hot-top needle (0.5-mm in diameter) or left unwounded. A noncolonized PDA plug was used to treat the control leaves. All the inoculated leaves were then placed in sterilized transparent containers (260 × 260 × 30 mm) with a layer of moist absorbent paper to maintain high relative humidity (RH). The containers were sealed with parafilm and maintained in a growth chamber at 25 °C with a 12 h photoperiod [33]. The experiment was conducted in three replicates for each treatment, and the entire experiment was repeated twice.

Plant inoculations were performed on newly developed leaves on potted seedlings of *C. paliurus* using the wounding method as described above. *C. paliurus* seedlings treated with noncolonized PDA plugs were used as controls. All the inoculated seedlings were subsequently placed in an incubator (25 °C, 12 h photoperiod, 90%–95% RH). Three replicates were performed for each treatment, and the entire experiment was repeated twice.

Inoculated leaves were monitored and recorded for symptom development of anthracnose for up to three weeks. Disease incidence (percentage of infected leaves) was evaluated at 10 days post inoculation (dpi), and severity was assessed by measuring lesion length in two perpendicular directions at 15 dpi. To fulfil Koch's postulates, all *Colletotrichum* isolates used in pathogenicity tests were reisolated from the infected leaves and their identity were confirmed according to cultural characteristics and GADPH sequences as described above. In addition, inoculated leaves bearing typical *Colletotrichum* conidial masses or ascomata were collected and prepared in accordance with Fu et al. [18]. Photomicrographs were taken under a ZEISS fluorescence microscope (Stereo Discovery V20, Carl Zeiss, Germany).

2.5. Data Analyses

The data used for the statistical analyses of the morphological characteristics and virulence of *Colletotrichum* species are presented as the mean ± standard error (SE) or standard deviation (SD) and were analyzed using Origin 2021. Differences between treatments were evaluated using one-way analysis of variance (ANOVA) in SPSS 26.0 software. When ANOVA revealed significant differences, the treatment means were compared according to Tukey's honestly significant difference test ($p = 0.05$).

3. Results

3.1. Symptomatology and Fungal Isolation

The typical symptoms of *C. paliurus* anthracnose observed in the present study were initially circular or irregularly shaped black-brown spots that gradually enlarged and then collapsed into necrotic lesions, turning grey, white or brown in the middle and dark brown at the edges (Figure 1A,B). Severe infection resulted in extensive early defoliation and eventually the death of the whole plant (Figure 1C). Under high-humidity conditions, typical structures of *Colletotrichum*, such as ascomata (Figure 1D), conidiomata (Figure 1E), and setae (Figure 1F), appeared on these lesions. In total, 337 isolates were recovered from symptomatic *C. paliurus* leaves that were collected in eight surveyed provinces of southern China. According to ITS sequence alignment, 331 isolates were identified as *Colletotrichum* spp. Other isolates belonging to *Pestalotiopsis*, *Alternaria* and *Phomopsis* were also isolated, but those were not further studied for the time being (Table A3).

3.2. Molecular Identification and Phylogenetic Analyses

Based on the alignment of ITS and GADPH sequences and cultural characteristics, all *Colletotrichum* isolates were grouped into the Gloeosporioides (249 isolates), Acutatum (37 isolates), Orchidearum (32 isolates) and Magnum complexes (13 isolates). Subsequently, a subset of 43 isolates representing different geographic origins, phenotypic characteristics (conidial shape and size) and genetic diversity (ITS and GADPH sequence analysis) was selected for further investigation (Tables A1 and A2).

For isolates in the Gloeosporioides complex, phylogenetic analyses of eight concatenated loci (ITS, *GADPH*, *CHS-1*, *ACT*, *TUB*, *CAL*, *GS* and *ApMat*) sequences were carried out with corresponding sequences from 39 authentic specimens (Table A1). The concatenated matrixes of the aligned dataset were composed of 3537 characters and gaps in the alignment. The GTR+G model was selected based on the AIC to reconstruct the ML tree.

For BI analysis, the corresponding models were selected by MrModeltest: GTR+I+G for ITS; K80+G for *GAPDH* and *ApMat*; HKY+I+G for *CHS-1*; and GTR+G for *ACT*, *TUB*, *CAL* and *GS*. The isolates in the Gloeosporioides complex were clustered into two well-supported clades (Bv > 99% and Bayesian PP = 1.00): 18 isolates were grouped into the *C. fructicola* clade, and five were clustered with *C. gloeosporioides* s. s. (Figure 2).

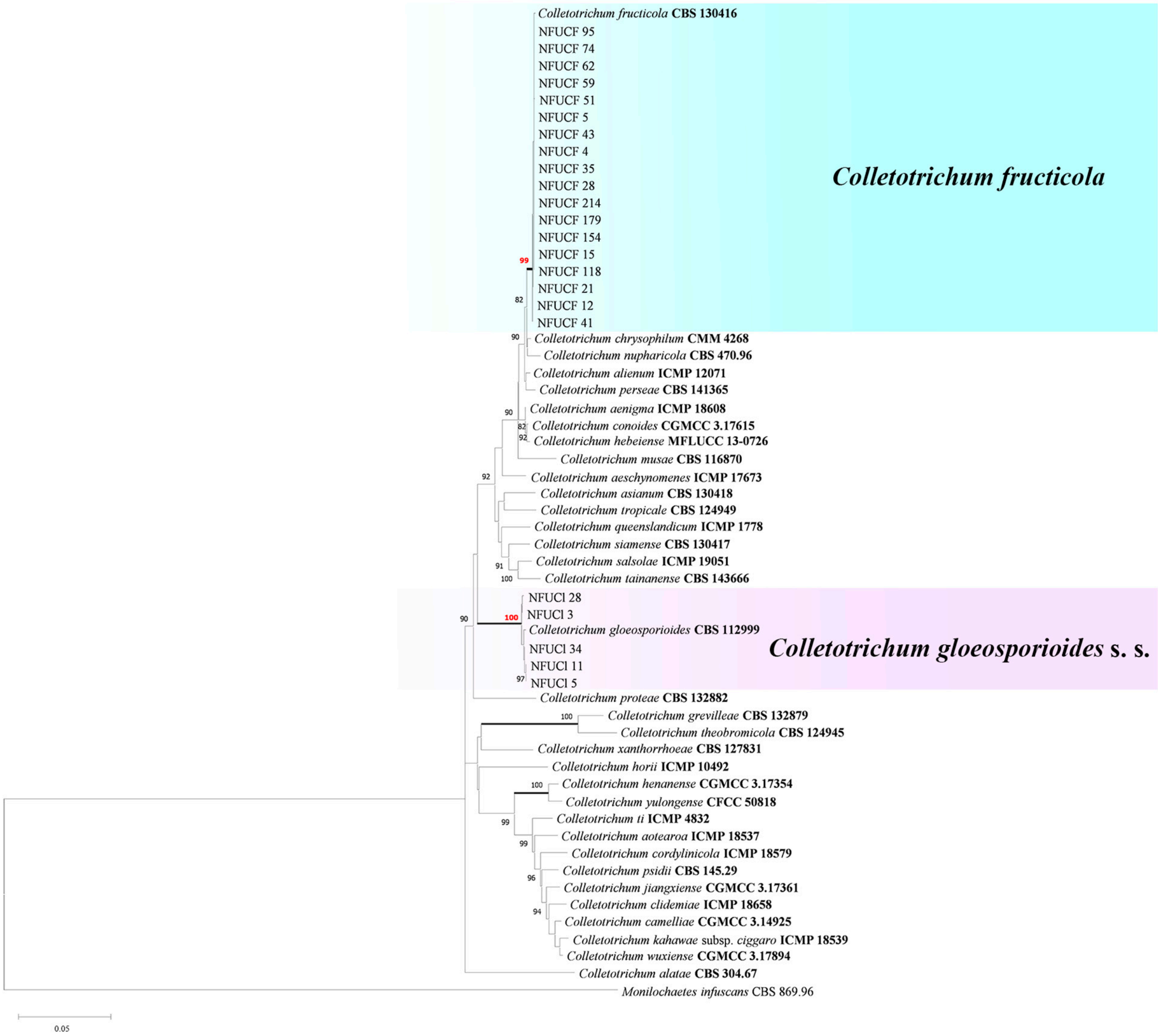

Figure 2. Phylogram tree inferred from a maximum likelihood analysis based on eight-gene combined dataset (ITS, *GADPH*, *CHS-1*, *ACT*, *TUB*, *CAL*, *GS* and *ApMat*) alignments of the *Colletotrichum gloeosporioides* species complex. Bootstrap support values (Bv) above 80% are shown at the nodes. Branches in bold represent strong support (posterior probability values = 1.00) confirmed by Bayesian analysis. Ex-type or other authoritative cultures are emphasized in bold font. The tree was rooted to *Monilochaetes infuscans* (CBS 869.96). The scale bar indicates the average number of expected changes per site.

To identify the *Colletotrichum* species within the Acutatum, Magnum and Orchidearum complexes, a dataset of six combined genes (ITS, *GADPH*, *CHS-1*, *ACT*, *TUB* and *HIS3*) from 49 authentic specimens was used, and the dataset comprised 1905 characters after alignment. The ML tree was reconstructed utilizing the GTR+G+I model. The best models for BI were found by MrModeltest: GTR+I+G for ITS, *CHS-1* and *HIS3*, K80+G for *GADPH*, GTR+G for *ACT*, and HKY+I+G for *TUB*. The isolates in the Acutatum complex could be well defined as *C. nymphaeae* and *C. godetiae* because five isolates clustered together with the *C. nymphaeae* ex-type strain CBS 515.78 with strong support (99% Bv/1.00 PP), and five isolates clustered in another highly supported clade (99% BP/1.00 PP) with the *C. godetiae* type strain CBS 133.44. Among the isolates in the Orchidearum complex, five were grouped in *C. plurivorum* Damm, Alizadeh & Toy. Sato (98% Bv/1.00 PP), whereas the other five isolates were clustered with *C. sojae* Damm & Alizadeh (99% Bv/1.00 PP). Additionally, the remaining five isolates clustered with the *C. brevisporum* authentic strain BCC 38876 with high support (99% Bv/1.00 PP) in the Magnum clade (Figure 3).

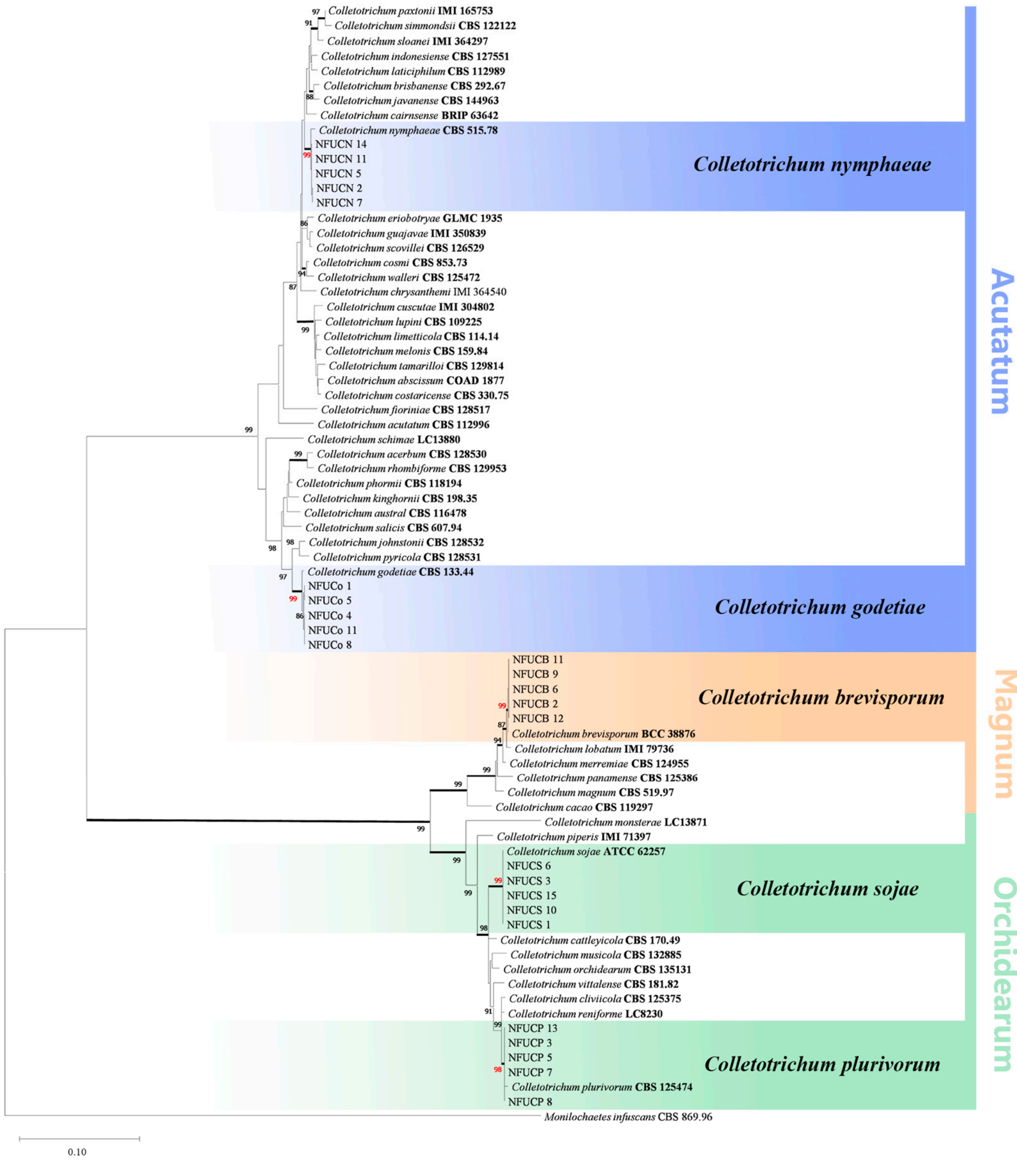

Figure 3. Phylogenetic tree resulting from maximum likelihood analysis using the six-gene combined dataset (ITS, *GADPH*, *CHS-1*, *ACT*, *TUB* and *HIS3*) alignments of the *Colletotrichum acutatum* (Acutatum), *C. magnum* (Magnum) and *C. orchidearum* (Orchidearum) species complexes. Bootstrap support values (Bv) above 80% are shown at the nodes. Branches in bold represent strong support (posterior probability values = 1.00) confirmed by Bayesian analysis. Ex-type or other authoritative cultures are emphasized in bold font. The tree was rooted with *Monilochaetes infuscans* (CBS 869.96). The scale bar indicates the average number of expected changes per site.

3.3. Morphological Characteristics

Colonies of *C. brevisporum* isolates on PDA were dark grey with grey aerial mycelium and edges (Figure 4). Yellowish conidial conidiomata formed across the colony after 14 days of incubation at 25 °C. The conidia were cylindrical to clavate, smooth-walled, hyaline, aseptate, and rounded at both ends (few one end rounded to acute), measuring 10.6 to 17.3 × 5.0 to 6.8 µm (average 14.1 ± 1.2 × 5.8 ± 0.3 µm). The appressoria were globose, puce, with an entire or lobed margin, and 7.5 to 17.5 × 5.6 to 13.2 µm (average 10.5 ± 1.7 × 8.9 ± 0.9 µm) in size (Table 2). Conidiophores and setae formed from a brown stroma. The setae were dark brown, straight to slightly curved, opaque, tip acute, and base cylindrical (Figure 4). The mycelial growth rate was 12.7 ± 0.2 mm per day on PDA at 25 °C (Table 2).

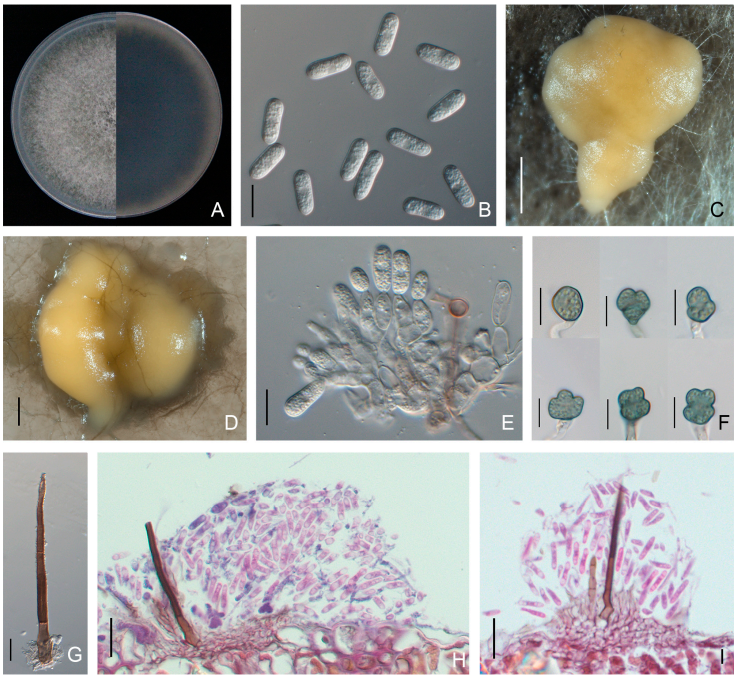

Figure 4. Morphological features of *Colletotrichum brevisporum* isolate NFUCB-6 from *Cyclocarya paliurus*: (**A**) front and back views of a 6-d-old PDA culture; (**B**) conidia; (**C**,**D**) conidiomata produced on PDA and SNA, respectively; (**E**) conidiophores; (**F**) appressoria; (**G**) setae; (**H**,**I**) section view of acervuli produced on a *Cyclocarya paliurus* leaf. Scale bars: (**B**,**E**–**G**) =10 µm; (**C**) =200 µm; (**D**) =500 µm; (**H**,**I**) =20 µm.

Colonies of *C. fructicola* isolates were olive-grey with whitish edges on PDA, and the average growth rate was 14.4 ± 0.2 mm/day. Conidia were produced as brick-red masses and were hyaline, smooth-walled, aseptate, cylindrical with rounded ends, and 10.3 to 22.5 × 4.4 to 7.9 µm (average 13.5 ± 1.8 × 5.8 ± 0.5 µm) in size. Conidiophores were hyaline, simple to 2-septate, and unbranched. Appressoria were greyish brown to black and formed singularly, with ovoid to slightly irregular outlines, measuring 6.5 to 16.0 × 4.5 to 9.1 µm (average 9.5 ± 1.6 × 7.0 ± 0.9 µm). Asci were clavate, fasciculate and 8-spored. Ascospores were smooth-walled, hyaline, aseptate, partly guttulate, curved fusoid with rounded ends and 12.3 to 23.2 × 3.8 to 6.5 µm (average 17.7 ± 1.7 × 5.0 ± 0.6 µm) in size (Figure 5, Table 2).

Table 2. Phenotypic and morphological characteristics of representative isolates from *Cyclocarya paliurus* of the seven *Colletotrichum* species identified in the present study.

Species	Colony Appearance	Growth Rate (mm/d) [a]	Conidia			Appressoria			Ascospores		
			Length (μm) [b]	Width (μm) [b]	Shape	Length (μm) [b]	Width (μm) [b]	Shape	Length (μm) [b]	Width (μm) [b]	Shape
Colletotrichum brevisporum	Dense, dark-grey with the grey aerial mycelium and edges	12.7 ± 0.2 B	14.1 ± 1.2 (10.6–17.3)	5.8 ± 0.3 (5.0–6.8)	Cylindrical	10.5 ± 1.7 (7.5–17.5)	8.9 ± 1.4 (5.6–13.2)	Globose, entire or lobed margin	/	/	/
C. fructicola	Dense, olive-grey with the white edge hyphae	14.4 ± 0.2 A	13.5 ± 1.8 (10.3–22.5)	5.8 ± 0.5 (4.4–7.9)	Cylindrical	9.5 ± 1.6 (6.5–16.0)	7.0 ± 0.9 (4.5–9.1)	Ovoid to slightly irregular	17.7 ± 1.7 (12.3–23.2)	5.0 ± 0.6 (3.8–6.5)	Curved fusoid
C. gloeosporioides	Dense, white with whitish aerial mycelium and edges	12.6 ± 0.5 B	15.9 ± 1.1 (13.1–22.7)	5.5 ± 0.4 (4.5–6.3)	Cylindrical	9.6 ± 1.0 (7.2–12.5)	7.2 ± 0.9 (6.0–10.3)	Ovoid to slightly irregular	/	/	/
C. godetiae	Dense, white hyphae, lack of aerial mycelium	8.4 ± 0.2 E	15.9 ± 1.3 (12.6–20.7)	5.1 ± 0.4 (3.8–6.8)	Fusiform	9.5 ± 1.0 (7.6–13.2)	6.4 ± 0.7 (4.9–8.7)	Ovoid to globose	/	/	/
C. nymphaeae	Dense, olive-grey with white margin, lack of aerial mycelium	9.8 ± 0.2 D	14.5 ± 1.9 (11.1–18.0)	5.5 ± 0.9 (4.0–6.9)	Fusiform	9.1 ± 1.3 (7.0–11.9)	7.0 ± 1.1 (5.0–8.9)	Ovoid, with smooth margin	/	/	/
C. plurivorum	Dense, olive-grey with the white edge hyphae	11.1 ± 0.1 C	14.9 ± 1.6 (12.1–20.2)	6.2 ± 0.6 (5.0–7.7)	Cylindrical	12.4 ± 2.2 (8.6–20.5)	9.2 ± 1.2 (6.4–12.5)	Globose, entire or lobed margin	18.0 ± 1.6 (13.6–23.0)	7.0 ± 0.8 (5.0–9.3)	Fusiform to curved fusoid
C. sojae	Dense, light orange-red with the whitish aerial mycelium and edges	14.7 ± 0.7 A	/	/	/	11.1 ± 1.7 (7.2–18.0)	7.4 ± 0.7 (5.7–9.4)	Ovoid, entire or lobed margin	24.4 ± 4.4 (13.2–32.1)	5.0 ± 0.7 (3.0–6.8)	Curved fusoid

[a] Data are mean ± standard deviation. Means with different letters indicate mean lesion lengths that are significantly different ($p < 0.05$). [b] Data are mean ± standard deviation, with ranges in parentheses. / means data were absent.

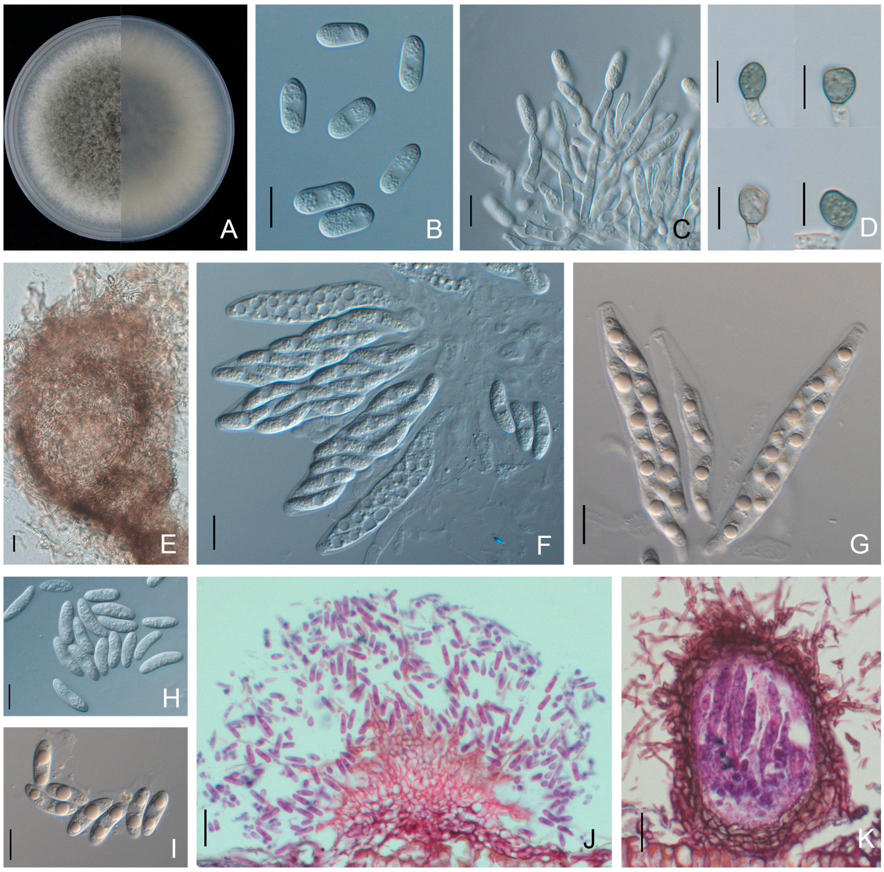

Figure 5. Morphological features of *Colletotrichum fructicola* isolate NFUCF-62 from *Cyclocarya paliurus*. (**A**) Front and back views of a 6-d-old PDA culture; (**B**) conidia; (**C**) conidiophores; (**D**) appressoria; (**E**) ascomata; (**F**,**G**) asci; (**H**,**I**) ascospores; (**J**,**K**) section view of acervuli and ascomata produced on a *Cyclocarya paliurus* leaf, respectively. Scale bars: (**B**–**D**,**F**–**I**) =10 µm; (**E**,**J**,**K**) =20 µm.

Colonies of *C. gloeosporioides* s. s. on PDA were white to off-white with dense aerial mycelia and edges, and the average growth rate was 12.6 ± 0.5 mm/day. Conidia were cylindrical, straight with a few slightly curved, aseptate, hyaline, rounded at both ends, and were 13.1 to 22.7 × 4.5 to 6.3 µm (average 15.9 ± 1.1 × 5.5 ± 0.4 µm) in size. Brown-colored appressoria were ovoid to slightly irregular, with an entire margin measuring 7.2 to 12.5 × 6.0 to 10.3 µm (average 9.6 ± 1.0 × 7.2 ± 0.9 µm) (Figure 6, Table 2). Conidiophores and setae formed from a dark brown stroma. Setae were dark brown, straight to slightly curved, and opaque, with acute tip and cylindrical base (Figure 6).

The *C. godetiae* isolates exhibited dense and white colonies on PDA, and the average growth rate was 8.4 ± 0.2 mm/day. Conidia were produced in orange conidiomata and were aseptate, hyaline and fusiform, with one end rounded and one end rounded to acute, measuring 12.6 to 20.7 × 3.8 to 6.8 µm (average 15.9 ± 1.3 × 5.1 ± 0.4 µm). Conidiophores and setae formed from a brown stroma. Setae were dark brown, straight or curved, and opaque, with acute tip and cylindrical base. Sexual morphs were not observed (Figure 7). Appressoria were greyish brown to black, ovoid to globose, with entire or lobed margins, and 7.6 to 13.2 × 4.9 to 8.7 µm (average 9.5 ± 1.0 × 6.4 ± 0.7 µm) in size (Figure 7, Table 2).

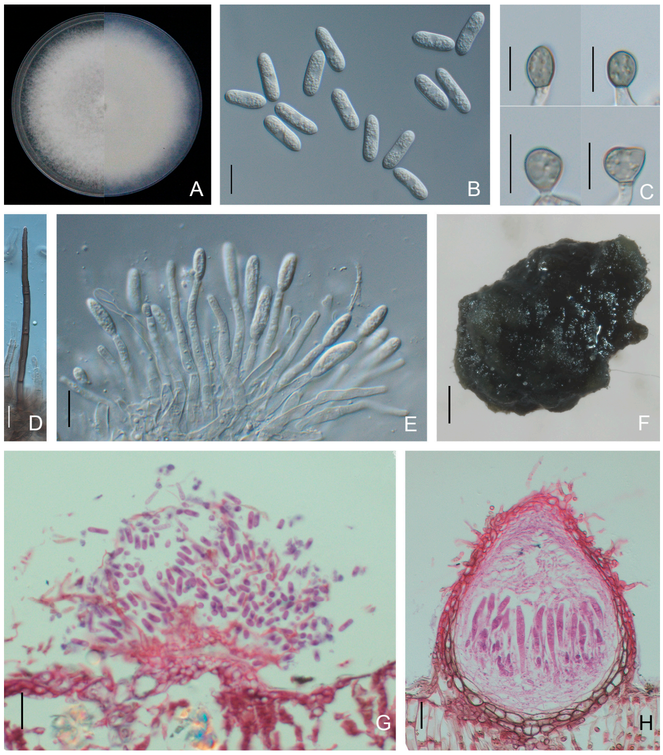

Figure 6. Morphological features of *Colletotrichum gloeosporioides* sensu stricto isolate NFUCl-5 from *Cyclocarya paliurus*. (**A**) Front and back views of a 6-d-old PDA culture; (**B**) conidia; (**C**) appressoria; (**D**) setae; (**E**) conidiophores; (**F**) conidiomata produced on SNA; (**G**,**H**) section view of acervuli and ascomata produced on a *Cyclocarya paliurus* leaf, respectively. Scale bars: (**B**–**E**) =10 µm; (**F**) =200 µm; (**G**,**H**) =20 µm.

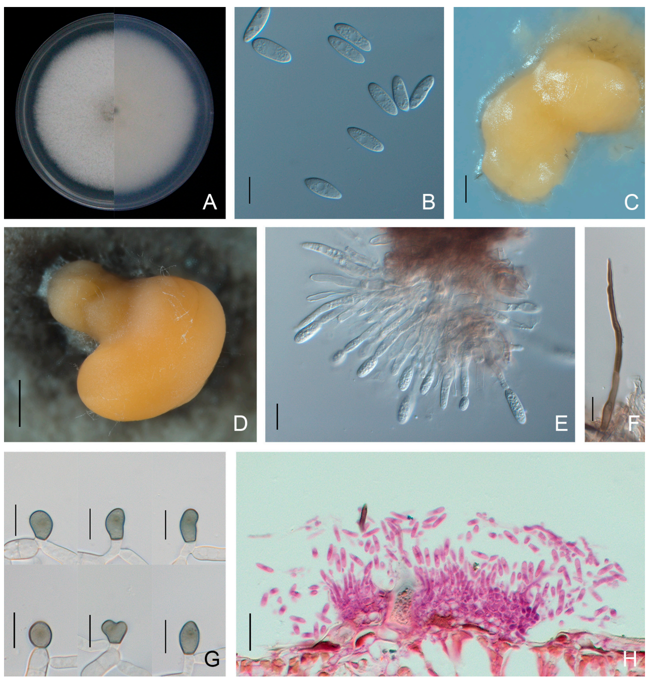

Figure 7. Morphological features of *Colletotrichum godetiae* isolate NFUCo-1 from *Cyclocarya paliurus*. (**A**) Front and back views of a 6-day-old PDA culture; (**B**) conidia; (**C**,**D**) conidiomata produced on SNA and PDA, respectively; (**E**) conidiophores; (**F**) setae; (**G**) appressoria; (**H**) section view of acervuli produced on a *Cyclocarya paliurus* leaf. Scale bars: (**B**,**E**–**G**) =10 µm; (**C**) =200 µm; (**D**) =500 µm; (**H**) =20 µm.

Colletotrichum nymphaeae colonies on PDA were dense, olive-grey with a white margin after 6 days of incubation, and had similar morphological features to those of *C. godetiae*. Conidia were fusiform with one end rounded and one end rounded to acute, measuring 11.1 to 18.0 × 4.0 to 6.9 µm (average 14.5 ± 1.9 × 5.5 ± 0.9 µm). Appressoria were greyish brown to black, ovoid, with smooth margins, and 7.0 to 11.9 × 5.0 to 8.9 µm (average 9.1 ± 1.3 × 7.0 ± 1.1 µm) in size (Figure 8, Table 2). The average growth rate of *Colletotrichum nymphaeae* isolates on PDA was 9.8 ± 0.2 mm per day (Table 2).

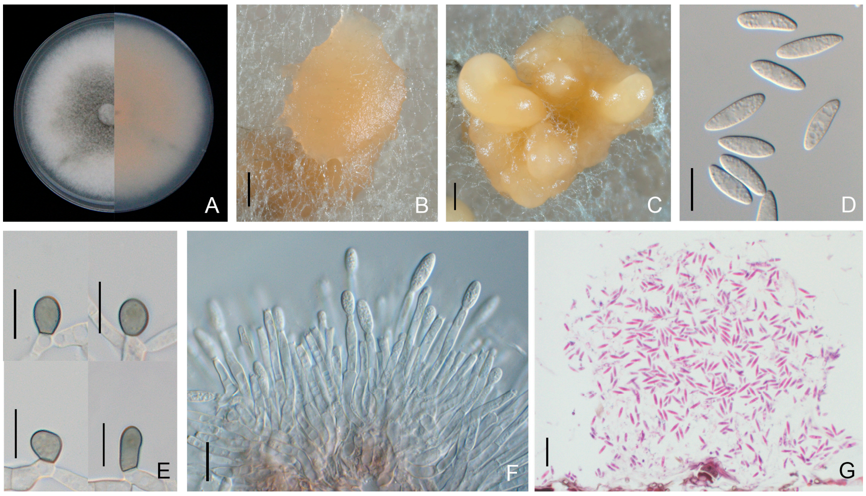

Figure 8. Morphological features of *Colletotrichum nymphaeae* isolate NFUCN-2 from *Cyclocarya paliurus*. (**A**) Front and back views of a 6-d-old PDA culture; (**B**,**C**) conidiomata produced on PDA and SNA, respectively; (**D**) conidia; (**E**) appressoria; (**F**) conidiophores; (**G**) sectional view of acervuli produced on a *Cyclocarya paliurus* leaf. Scale bars: (**B**,**C**) =200 µm; (**D**–**F**) =10 µm; (**G**) =20 µm.

Colonies of *C. plurivorum* isolates on PDA were olive-grey with white margins, and the average growth rate was 11.1 ± 0.1 mm/day. Conidia were aseptate, hyaline, cylindrical with rounded ends, and 12.1 to 20.2 × 5.0 to 7.7 µm (average 14.9 ± 1.6 × 6.2 ± 0.6 µm) in size. Conidiophores were hyaline, unbranched, and formed from a brown stroma. Setae were dark brown, straight and opaque, with acute tip and cylindrical base (Figure 9). Appressoria were globose to ovoid, puce, with an entire or lobed margin, and 8.6 to 20.5 × 6.4 to 12.5 µm (average 12.4 ± 2.2 × 9.2 ± 1.2 µm) in size. Ascomata were semi-immersed in agar medium, subglobose to pyriform, and dark brown. Asci were clavate or fasciculate, and eight-spored (Figure 9). Ascospores were hyaline, smooth-walled, aseptate, fusiform to curved fusoid, and rounded at both ends, measuring 13.6 to 23.0 × 5.0 to 9.3 µm (average 18.0 ± 1.6 × 7.0 ± 0.8 µm) (Figure 9, Table 2).

Colletotrichum sojae colonies on PDA were light orange-red with whitish aerial mycelia and edges, and the average growth rate was 14.7 ± 0.7 mm per day. Asexual morphs were not observed. Ascomata formed on PDA or SNA after two weeks of inoculation, which were subglobose to pyriform, dark brown, ostiolate, and semi-immersed in the agar medium. Asci were clavate or fasciculate and eight-spored (Figure 10). Ascospores were hyaline, aseptate, smooth-walled and curved fusoid with rounded ends, had granular content and measured 13.2 to 32.1 × 3.0 to 6.8 µm (average 24.4 ± 4.4 × 5.0 ± 0.7 µm). Appressoria were puce, ovoid with an entire or lobed margin and 7.2 to 18.0 × 5.7 to 9.4 µm (average 11.1 ± 1.7 × 7.4 ± 0.7 µm) in size (Figure 10, Table 2).

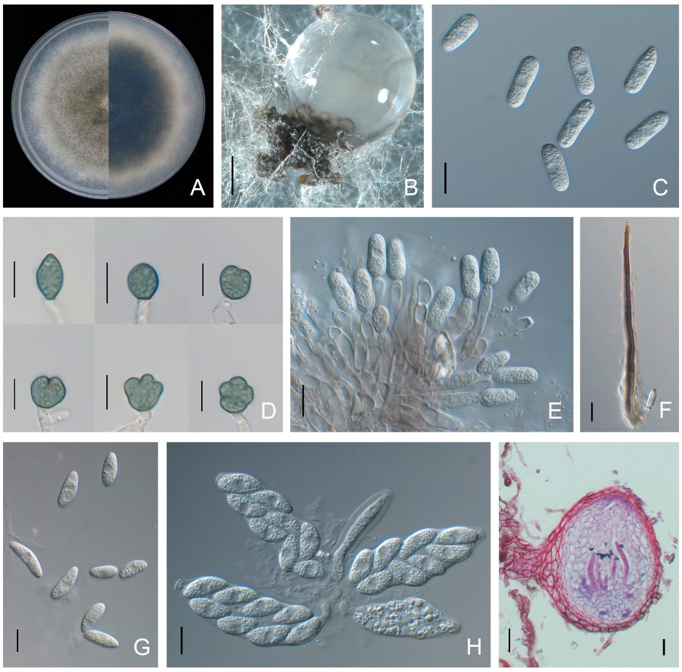

Figure 9. Morphological features of *Colletotrichum plurivorum* isolate NFUCP-13 from *Cyclocarya paliurus*. (**A**) Front and back view of 6-day-old PDA culture; (**B**) ascomata produced on SNA; (**C**) conidia; (**D**) appressoria; (**E**) conidiophores; (**F**) setae; (**G**) ascospores; (**H**) asci; (**I**) section view of ascomata produced on *Cyclocarya paliurus* leaf. Scale bars: (**B**) =500 µm; (**C**–**H**) =10 µm; (**I**) =20 µm.

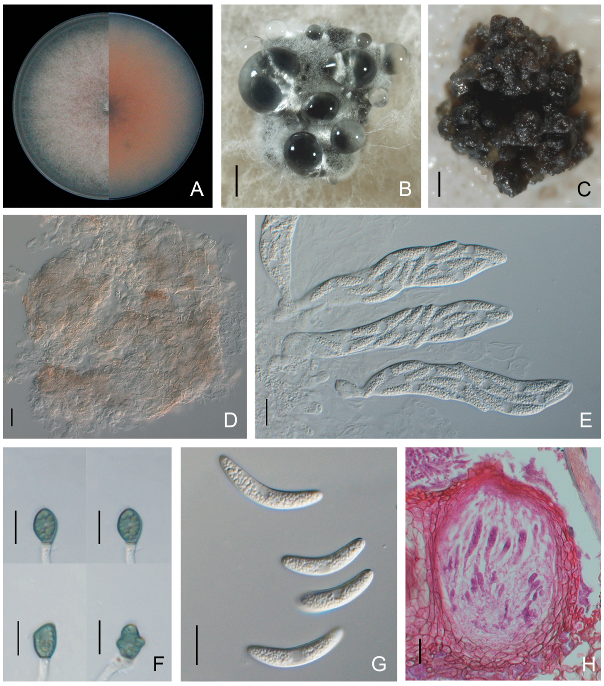

Figure 10. Morphological features of *Colletotrichum sojae* isolate NFUCS-10 from *Cyclocarya paliurus*. (**A**) Front and back views of a 6-day-old PDA culture; (**B**,**C**) ascomata produced on PDA and SNA, respectively; (**D**) ascomata; (**E**) asci; (**F**) appressoria; (**G**) ascospores; (**H**) section view of ascomata produced on a *Cyclocarya paliurus* leaf. Scale bars: (**B**) =500 µm; (**C**) =200 µm; (**D**,**H**) =20 µm; (**E**–**G**) =10 µm.

3.4. Pathogenicity Tests

The data from the pathogenicity tests are given in Table 3. Representative isolates of all seven *Colletotrichum* species produced typical symptoms of anthracnose on detached *C. paliurus* leaves, while the corresponding mock controls remained asymptomatic up to 10 dpi. Inoculation with *C. fructicola*, *C. godetiae*, *C. gloeosporioides* s. s., *C. nymphaeae* and *C. sojae* isolates led to the development of anthracnose symptoms on leaves through both wounding and nonwounding methods, whereas *C. brevisporum* and *C. plurivorum* ones exhibited weaker virulence and were only capable of infecting wounded leaves.

Table 3. Results of pathogenicity tests of *Colletotrichum* isolates artificially inoculated on *Cyclocarya paliurus*.

Species	Detached Leaves [a]				Intact Plant [a]	
	Wounding		Nonwounding		Wounding	
	Disease Incidence (%)	Lesion Diameter (cm)	Disease Incidence (%)	Lesion Diameter (cm)	Disease Incidence (%)	Lesion Diameter (cm)
Colletotrichum brevisporum	66.7 ± 10.3	5.4 ± 1.1 D	–	–	–	–
C. fructicola	100.0 ± 0.0	25.3 ± 0.8 A	100.0 ± 0.0	20.1 ± 1.3 a	88.7 ± 7.2	9.4 ± 1.0 a
C. gloeosporioides	100.0 ± 0.0	18.0 ± 1.0 B	100.0 ± 0.0	17.7 ± 0.9 a	66.7 ± 8.7	6.2 ± 1.1 ab
C. godetiae	100.0 ± 0.0	21.8 ± 1.0 AB	100.0 ± 0.0	16.9 ± 1.2 a	66.3 ± 12.2	6.1 ± 1.1 ab
C. nymphaeae	100.0 ± 0.0	19.2 ± 0.7 B	55.2 ± 11.1	3.6 ± 0.8 b	33.0 ± 12.0	2.3 ± 0.9 b
C. plurivorum	66.2 ± 8.7	6.6 ± 1.2 CD	–	–	–	–
C. sojae	100.0 ± 0.0	10.4 ± 0.7 C	38.5 ± 13.2	2.3 ± 0.7 b	–	–

[a] Data are means (±standard error) of two repeated experiments. Means with different letters indicate mean lesion lengths that are significantly different ($p < 0.05$). – indicates no symptom developed on inoculated site.

All isolates of *Colletotrichum* species showed a higher incidence and severity of disease on wounded leaves than on nonwounded leaves. Moreover, the isolates of the different species displayed distinct levels of aggressiveness. Among them, isolates of *C. fructicola* exhibited the highest aggressiveness on both detached leaves and intact plants. At 3 dpi, symptoms began to appear around the inoculation site, and then the lesion expanded rapidly. Dark-brown necrotic lesions were observed with typical *Colletotrichum* acervuli or ascomata after 15 dpi. The average lesion diameters (mean ± SE) were 25.3 ± 0.8 mm, 20.1 ± 1.3 mm and 9.4 ± 1.0 mm on wounded detached leaves, nonwounded detached leaves and intact plants, respectively. The virulence of *C. gloeosporioides* s. s., *C. godetiae* and *C. nymphaeae* isolates was weaker than that of *C. fructicola* isolates. In contrast, *C. brevisporum*, *C. plurivorum* and *C. sojae* were weakly aggressive to *C. paliurus* leaves, and at 15 dpi, the symptoms on nonwounded leaves and intact plants did not markedly spread or remained asymptomatic. There was no significant difference in pathogenicity between different strains of the same *Colletotrichum* species. Re-isolation from infected leaves was successful and confirmed by morphological and molecular identification, thus fulfilling Koch's postulates.

4. Discussion

Anthracnose is the most prevalent foliar disease in all major *C. paliurus*-growing areas in southern China, causing enormous pecuniary losses under humid conditions and disease-favorable temperatures. Unfortunately, the species diversity of *C. paliurus* anthracnose pathogens in southern China remains largely unclear. In the present study, we collected and characterized 331 *Colletotrichum* isolates from eight *C. paliurus* planting provinces and identified seven species belonging to the Gloeosporioides, Acutatum, Magnum and Orchidearum complexes, demonstrating that diverse *Colletotrichum* species complexes can infect *C. paliurus*.

The ascomycete genus *Colletotrichum* includes important phytopathogens that cause anthracnose worldwide. Among them, three species belonging to the Gloeosporioides complex have been identified to induce *C. paliurus* anthracnose in China [10], whereas

C. fructicola and *C. gloeosporioides* s. s. were identified in this study. The composition of *Colletotrichum* spp. causing *C. paliurus* anthracnose has been reported only in Jiangsu Province, where the Gloeosporioides complex was consistently reported as the most dominant instigator. Nevertheless, based on extensively collected samples, we found that the Gloeosporioides complex was not the only species complex causing *C. paliurus* anthracnose.

Taxonomic studies of *Colletotrichum* species have focused on disentangling intraspecific or specific taxa, traditionally according to phenotypic differences, mainly characteristics of cultural morphology, growth rate and microstructure morphs [34,35]. However, environmental factors and cultural conditions have major impacts on the stability of phenotypic traits. Furthermore, the morphological characteristics of *Colletotrichum* spp. within the species complex largely overlap; thus, phenotypical criteria are not adequate for a precise identification [34].

In terms of molecular characterization, for several fungi, the ITS region has been proposed as a universal DNA marker [36]; however, previous studies have proven that *Colletotrichum* species cannot be efficiently distinguished by ITS alone. Consequently, other loci such as *GADPH*, *GS* and *ApMat* must be considered. Hyde et al. [37] suggested that the *GADPH* gene is the most variable marker across multiple *Colletotrichum* species complexes. Several studies have recommended the use of the *ApMat* marker for the delimitation of cryptic species within the Gloeosporioides complex, yet Tovar-Pedraza [38] reported that *C. jiangxiense* and *C. kahawae* in the Gloeosporioides complex cannot be distinguished from each other by only *ApMat* sequence data, and their identification requires *GS*- and *ApMat*-concatenated phylogenetic analysis. In the present work, phylogenetic analyses of eight loci (ITS, *GAPDH*, *ACT*, *CHS-1*, *TUB*, *CAL*, *GS* and *ApMat*) in the Gloeosporioides complex and six loci (ITS, *GAPDH*, *ACT*, *CHS-1*, *TUB*, *CAL* and *HIS3*) in the other species complexes revealed that 43 representative isolates belonged to seven known *Colletotrichum* species, including *C. brevisporum*, *C. fructicola*, *C. gloeosporioides* s. s., *C. godetiae*, *C. nymphaeae*, *C. plurivorum* and *C. sojae* (Figures 2 and 3). Furthermore, the morphological groups identified based on colony features, asexual or sexual morphs, and typical *Colletotrichum* conidial masses or ascomata that developed on inoculated leaves were entirely consistent with the results of the molecular data.

Pathogenicity tests revealed that all seven *Colletotrichum* species were pathogenic to wounding detached leaves of *C. paliurus*. When the foliar tissue was wounded, the incidence and severity of disease increased significantly. These results suggest that wounds may play an important role for pathogen penetration into the host. On average, species within the Gloeosporioides and Acutatum complexes produced larger lesions than those in the Magnum and Orchidearum complexes, which may be one of the notable factors contributing to the prevalence of the Gloeosporioides complex. Moreover, different *Colletotrichum* species had various degrees of aggressiveness on *C. paliurus* leaves. *C. fructicola* in the Gloeosporioides complex was the most aggressive species. Thus, a species-specific diagnosis is highly important for the prediction of relative aggressiveness; the species complex alone is not a sufficient indicator of pathogenicity or disease risk.

A previous study demonstrated that *C. fructicola* was the most common pathogen causing *C. paliurus* anthracnose in Jiangsu Province, China [10]. Similarly, in the present work, the dominant causal agent associated with *C. paliurus* anthracnose was *C. fructicola* on the basis of the highest isolation rate and aggressiveness levels. *C. fructicola* was originally isolated from coffee berries in Thailand [39]. It has been subsequently reported that *C. fructicola* could cause serious anthracnose infections in Australia, Brazil, China, Malaysia and the USA [18,40–43]. *C. fructicola* has been found on a broad range of host plants, such as fruit trees and economically important crops, including apple (*Malus* spp.), *Citrus* spp., mango (*Mangifera indica*), peach (*Prunus persica*), pear (*Pyrus* spp.), strawberry (Fragaria × ananassa) and tea (*Camellia sinensis*), possibly due to its parasitic and endophytic lifestyle [18,40,44–49].

5. Conclusions

This study presents the first large-scale survey of *Colletotrichum* species associated with *C. paliurus* anthracnose in southern China. It offers novel insights into the disease's aetiology, including the first report of *C. brevisporum*, *C. godetiae*, *C. nymphaeae*, *C. plurivorum* and *C. sojae* associated with *C. paliurus* anthracnose. Considering the occurrence of several species involved in *C. paliurus* anthracnose, future research should take into account that the effective control of this disease may depend on the individual characteristics of each *Colletotrichum* species and their distribution in the *C. paliurus* planting areas. Furthermore, in view of the dominance of *C. fructicola* in major planting regions and its greater aggressiveness than other species, more epidemiological studies are needed to elucidate this pathological system.

Author Contributions: Conceptualization, F.-M.C.; methodology, X.-R.Z.; software, X.-R.Z.; validation, M.-J.Z.; formal analysis, M.-J.Z.; investigation, X.-R.Z.; resources, F.-M.C.; data curation, M.-J.Z.; writing—original draft preparation, X.-R.Z.; writing—review and editing, X.-R.Z. and M.-J.Z.; visualization, X.-R.Z. and M.-J.Z.; supervision, F.-M.C.; project administration, F.-M.C.; funding acquisition, F.-M.C. All authors have read and agreed to the published version of the manuscript.

Funding: This research was funded by Postgraduate Research and Practice Innovation Program of Jiangsu Province, grant number KYCX20_0875 and KYCX23_1222.

Data Availability Statement: Data are contained within the article and Appendix A.

Conflicts of Interest: The authors declare no conflict of interest.

Appendix A

Table A1. Isolates of *Colletotrichum* from leaves of wheel wingnut and various hosts examined in this study.

Species	Culture/ Isolate [a]	Host	Location	GenBank Accession Number [b]							
				ITS	*GAPDH*	*CHS*	*ACT*	*TUB*	*CAL*	*GS*	*ApMat*
Colletotrichum aenigma	**ICMP 18608**	*Persea americana*	Israel	JX010244	JX010044	JX009774	JX009443	JX010389	JX009683	JX010078	KM360143
C. aeschynomenes	**ICMP 17673**	*Aeschynomene virginica*	USA	JX010176	JX009930	JX009799	JX009483	JX010392	JX009721	JX010081	KM360145
C. alatae	**CBS 304.67**	*Dioscorea alata*	India	JX010190	JX009990	JX009837	JX009471	JX010383	JX009738	JX010065	KC888932
C. alienum	**ICMP 12071**	*Malus domestica*	New Zealand	JX010251	JX010028	JX009882	JX009572	JX010411	JX009654	JX010101	KM360144
C. aotearoa	**ICMP 18537**	*Coprosma* sp.	New Zealand	JX010205	JX010005	JX009853	JX009564	JX010420	JX009611	JX010113	KC888930
C. asianum	**CBS 130418**	*Coffea arabica*	Thailand	FJ972612	JX010053	JX009867	JX009584	JX010406	FJ917506	JX010096	FR718814
C. camelliae	**CGMCC 3.14925**	*Camellia sinensis*	China	KJ955081	KJ954782	MZ799255	KJ954363	KJ955230	KJ954634	KJ954932	KJ954497
C. chrysophilum	**CMM 4268**	*Musa* sp.	Brazil	KX094252	KX094183	KX094083	KX093982	KX094285	KX094063	KX094204	KX094325
C. clidemiae	**ICMP 18658**	*Clidemia hirta*	USA	JX010265	JX009989	JX009877	JX009537	JX010438	JX009645	JX010129	KC888929
C. conoides	**CGMCC 3.17615**	*Chili pepper*	China	KP890168	KP890162	KP890156	KP890144	KP890174	KP890150	-	-
C. cordylinicola	**ICMP 18579**	*Cordyline fruticosa*	Thailand	JX010226	JX009975	JX009864	HM470235	JX010440	HM470238	JX010122	JQ899274
C. fructicola	**CBS 130416**	*Coffea arabica*	Thailand	JX010165	JX010033	JX009866	FJ907426	JX010405	FJ917508	JX010095	JQ807838
	NFUCF-4	*Cyclocarya paliurus*	Sichuan, China	*OR056200*	*OR069484*	*OR073817*	*OR096449*	*OR073835*	*OR096522*	*OR098645*	*OR105821*
	NFUCF-5	*Cy. paliurus*	Guizhou, China	*OR056201*	*OR069485*	*OR073818*	*OR096450*	*OR073836*	*OR096523*	*OR098646*	*OR105822*
	NFUCF-12	*Cy. paliurus*	Sichuan, China	*OR056202*	*OR069486*	*OR073819*	*OR096451*	*OR073837*	*OR096524*	*OR098647*	*OR105823*

Table A1. *Cont.*

Species	Culture/ Isolate [a]	Host	Location	GenBank Accession Number [b]							
				ITS	*GAPDH*	*CHS*	*ACT*	*TUB*	*CAL*	*GS*	*ApMat*
	NFUCF-15 [c]	*Cy. paliurus*	Guangxi, China	*OR056203*	*OR069487*	*OR073820*	*OR096452*	*OR073838*	*OR096525*	*OR098648*	*OR105824*
	NFUCF-21	*Cy. paliurus*	Fujian, China	*OR056204*	*OR069488*	*OR073821*	*OR096453*	*OR073839*	*OR096526*	*OR098649*	*OR105825*
	NFUCF-28	*Cy. paliurus*	Hubei, Chna	*OR056205*	*OR069489*	*OR073822*	*OR096454*	*OR073840*	*OR096527*	*OR098650*	*OR105826*
	NFUCF-35	*Cy. paliurus*	Jiangxi, China	*OR056206*	*OR069490*	*OR073823*	*OR096455*	*OR073841*	*OR096528*	*OR098651*	*OR105827*
	NFUCF-41	*Cy. paliurus*	Guangxi, China	*OR056207*	*OR069491*	*OR073824*	*OR096456*	*OR073842*	*OR096529*	*OR098652*	*OR105828*
	NFUCF-43	*Cy. paliurus*	Fujian, China	*OR056208*	*OR069492*	*OR073825*	*OR096457*	*OR073843*	*OR096530*	*OR098653*	*OR105829*
	NFUCF-51	*Cy. paliurus*	Jiangxi, China	*OR056209*	*OR069493*	*OR073826*	*OR096458*	*OR073844*	*OR096531*	*OR098654*	*OR105830*
	NFUCF-59	*Cy. paliurus*	Guizhou, China	*OR056210*	*OR069494*	*OR073827*	*OR096459*	*OR073845*	*OR096532*	*OR098655*	*OR105831*
	NFUCF-62 [c]	*Cy. paliurus*	Hunan, China	*OR056211*	*OR069495*	*OR073828*	*OR096460*	*OR073846*	*OR096533*	*OR098656*	*OR105832*
	NFUCF-74	*Cy. paliurus*	Guangxi, China	*OR056212*	*OR069496*	*OR073829*	*OR096461*	*OR073847*	*OR096534*	*OR098657*	*OR105833*
	NFUCF-95	*Cy. paliurus*	Zhejiang, China	*OR056213*	*OR069497*	*OR073830*	*OR096462*	*OR073848*	*OR096535*	*OR098658*	*OR105834*
	NFUCF-118	*Cy. paliurus*	Guizhou, China	*OR056214*	*OR069498*	*OR073831*	*OR096463*	*OR073849*	*OR096536*	*OR098659*	*OR105835*
	NFUCF-154	*Cy. paliurus*	Hunan, China	*OR056215*	*OR069499*	*OR073832*	*OR096464*	*OR073850*	*OR096537*	*OR098660*	*OR105836*
	NFUCF-179	*Cy. paliurus*	Jiangxi, China	*OR056216*	*OR069500*	*OR073833*	*OR096465*	*OR073851*	*OR096538*	*OR098661*	*OR105837*
	NFUCF-214 [c]	*Cy. paliurus*	Zhejiang, China	*OR056217*	*OR069501*	*OR073834*	*OR096466*	*OR073852*	*OR096539*	*OR098662*	*OR105838*
C. gloeosporioides	**CBS 112999**	*Citrus sinensis*	Italy	JX010152	JX010056	JX009818	JX009531	JX010445	JX009731	JX010085	JQ807843
	NFUCl-3	*Cy. paliurus*	Guangxi, China	*OR064046*	*OR069502*	*OR073853*	*OR096419*	*OR096467*	*OR096540*	*OR098663*	*OR105839*
	NFUCl-5 [c]	*Cy. paliurus*	Jiangxi, China	*OR064047*	*OR069503*	*OR073854*	*OR096420*	*OR096468*	*OR096541*	*OR098664*	*OR105840*
	NFUCl-11 [c]	*Cy. paliurus*	Guizhou, China	*OR064048*	*OR069504*	*OR073855*	*OR096421*	*OR096469*	*OR096542*	*OR098665*	*OR105841*
	NFUCl-28	*Cy. paliurus*	Guizhou, China	*OR064049*	*OR069505*	*OR073856*	*OR096422*	*OR096470*	*OR096543*	*OR098666*	*OR105842*
	NFUCl-34 [c]	*Cy. paliurus*	Hunan, China	*OR064050*	*OR069506*	*OR073857*	*OR096423*	*OR096471*	*OR096544*	*OR098667*	*OR105843*
C. grevilleae	**CBS 132879**	*Grevillea* sp.	Italy	KC297078	KC297010	KC296987	KC296941	KC297102	KC296963	KC297033	-
C. hebeiense	**MFLUCC13–0726**	*Vitis vinifera*	China	KF156863	KF377495	KF289008	KF377532	KF288975	-	-	-
C. henanense	**CGMCC 3.17354**	*Ca. sinensis*	China	KJ955109	KJ954810	MZ799256	KM023257	KJ955257	KJ954662	KJ954960	KJ954524
C. horii	**ICMP 10492**	*Diospyros kaki*	Japan	GQ329690	GQ329681	JX009752	JX009438	JX010450	JX009604	JX010137	JQ807840
C. jiangxiense	**CGMCC 3.17361**	*Ca. sinensis*	China	KJ955149	KJ954850	MZ799257	KJ954427	OK236389	KJ954701	KJ955000	KJ954561
C. kahawae subsp. *ciggaro*	**ICMP 18539**	*Olea europaea*	Australia	JX010230	JX009966	JX009800	JX009523	JX010434	JX009635	JX010132	-
C. musae	**CBS 116870**	*Musa* sp.	USA	JX010146	JX010050	JX009896	JX009433	HQ596280	JX009742	JX010103	KC888926
C. nupharicola	**CBS 470.96**	*Nuphar lutea*	USA	JX010187	JX009972	JX009835	JX009437	JX010398	JX009663	JX010088	JX145319
C. perseae	**CBS 141365**	Avocado	Israel	KX620308	KX620242	MZ799260	KX620145	KX620341	KX620206	KX620275	KX620177
C. proteae	**CBS 132882**	*Protea* sp.	South Africa	KC297079	KC297009	KC296986	KC296940	KC297101	KC296960	KC297032	-
C. psidii	**CBS 145.29**	*Psidium* sp.	Italy	JX010219	JX009967	JX009901	JX009515	JX010443	JX009743	JX010133	KC888931
C. queenslandicum	**ICMP 1778**	*Carica papaya*	Australia	JX010276	JX009934	JX009899	JX009447	JX010414	JX009691	JX010104	KC888928
C. salsolae	**ICMP 19051**	*Salsola tragus*	Hungary	JX010242	JX009916	JX009863	JX009562	JX010403	JX009696	JX010093	KC888925
C. siamense	**CBS 130417**	*Coffea arabica*	Thailand	JX010171	JX009924	JX009865	FJ907423	JX010404	FJ917505	JX010094	JQ899289
C. tainanense	**CBS 143666**	*Capsicum annuum*	China	MH728818	MH728823	MH805845	MH781475	MH846558	-	MH748259	MH728836
C. theobromicola	**CBS 124945**	*Theobroma cacao*	Panama	JX010294	JX010006	JX009869	JX009444	JX010447	JX009591	JX010139	KC790726

Table A1. *Cont.*

Species	Culture/ Isolate [a]	Host	Location	GenBank Accession Number [b]							
				ITS	*GAPDH*	*CHS*	*ACT*	*TUB*	*CAL*	*GS*	*ApMat*
C. ti	**ICMP 4832**	*Cordyline* sp.	New Zealand	JX010269	JX009952	JX009898	JX009520	JX010442	JX009649	JX010123	KM360146
C. tropicale	**CBS 124949**	*Theobroma cacao*	Panama	JX010264	JX010007	JX009870	JX009489	JX010407	JX009719	JX010097	KC790728
C. wuxiense	**CGMCC 3.17894**	*Camellia sinensis*	China	KU251591	KU252045	KU251939	KU251672	KU252200	KU251833	KU252101	KU251722
C. xanthor-rhoeae	**CBS 127831**	*Xanthorrhoea preissii*	Australia	JX010261	JX009927	JX009823	JX009478	JX010448	JX009653	JX010138	KC790689
C. yulongense	**CFCC 50818**	*Vaccinium dunalianum*	China	MH751507	MK108986	MH793605	MH777394	MK108987	MH793604	MK108988	-
Monilochaetes infuscans	CBS 869.96	*Ipomoea batatas*	South Africa	JQ005780	JX546612	JQ005801	JQ005843	JQ005864	-	-	-

[a] Culture numbers in bold type represent ex-type or other authentic specimens. CBS 869.96 (*Monilochaetes infuscans*) was added as an outgroup. [b] Sequences in italics were generated in this study. "-"indicates missing data. [c] Isolates used for macroscopic and microscopic characterization and virulence tests.

Table A2. Strains of *Colletotrichum* excluded from the *C. gloeosporioides* species complex. Details are provided about clade, host and location, and GenBank accessions of the sequences generated.

Species	Culture/ Isolate [a]	Clade	Host	Location	GenBank Accession Number [b]					
					ITS	*GAPDH*	*CHS-1*	*HIS3*	*ACT*	*TUB2*
C. abscissum	**COAD 1877**	Acutatum	*Citrus sinensis* cv. *Pera*	Brazil	KP843126	KP843129	KP843132	KP843138	KP843141	KP843135
C. acerbum	**CBS 128530**	Acutatum	*Malus domestica*	New Zealand	JQ948459	JQ948790	JQ949120	JQ949450	JQ949780	JQ950110
C. acutatum	**CBS 112996**	Acutatum	*Carica papaya*	Australia	JQ005776	JQ948677	JQ005797	JQ005818	JQ005839	JQ005860
C. australe	**CBS 116478**	Acutatum	*Trachycarpus fortunei*	South Africa	JQ948455	JQ948786	JQ949116	JQ949446	JQ949776	JQ950106
C. brevisporum	**BCC 38876**	Magnum	*Neoregalia* sp.	Thailand	JN050238	JN050227	MZ799287	MZ673841	JN050216	JN050244
	NFUCB-2 [c]	Magnum	*Cyclocarya paliurus*	Hunan, China	*OR064061*	*OR069517*	*OR073868*	*OR096507*	*OR096434*	*OR096482*
	NFUCB-6 [c]	Magnum	*Cy. Paliurus*	Hunan, China	*OR064062*	*OR069518*	*OR073869*	*OR096508*	*OR096435*	*OR096483*
	NFUCB-9	Magnum	*Cy. Paliurus*	Hunan, China	*OR064063*	*OR069519*	*OR073870*	*OR096509*	*OR096436*	*OR096484*
	NFUCB-11	Magnum	*Cy. Paliurus*	Hunan, China	*OR064064*	*OR069520*	*OR073871*	*OR096510*	*OR096437*	*OR096485*
	NFUCB-12 [c]	Magnum	*Cy. Paliurus*	Guizhou, China	*OR064065*	*OR069521*	*OR073872*	*OR096511*	*OR096438*	*OR096486*
C. brisbanense	**CBS 292.67**	Acutatum	*Capsicum annuum*	Australia	JQ948291	JQ948621	JQ948952	JQ949282	JQ949612	JQ949942
C. cacao	**CBS 119297**	Magnum	*Theobroma cacao*	Costa Rica	MG600772	MG600832	MG600878	MG600916	MG600976	MG601039
C. cairnsense	**BRIP 63642**	Acutatum	*Capsicum annuum*	Australia	KU923672	KU923704	KU923710	KU923722	KU923716	KU923688
C. cattleyicola	**CBS 170.49**	Orchidearum	*Cattleya* sp.	Belgium	MG600758	MG600819	MG600866	MG600905	MG600963	MG601025
C. chrysanthemi	IMI 364540	Acutatum	*Chrysanthemum coronarium*	China	JQ948273	JQ948603	JQ948934	JQ949264	JQ949594	JQ949924
C. cliviicola	**CBS 125375**	Orchidearum	*Clivia miniata*	China	MG600733	MG600795	MG600850	MG600892	MG600939	MG601000
C. cosmi	**CBS 853.73**	Acutatum	*Cosmos* sp.	Netherlands	JQ948274	JQ948604	JQ948935	JQ949265	JQ949595	JQ949925
C. costaricense	**CBS 330.75**	Acutatum	*Coffea arabica*, cv. *Typica*	Costa Rica	JQ948180	JQ948510	JQ948841	JQ949171	JQ949501	JQ949831
C. cuscutae	**IMI 304802**	Acutatum	*Cuscuta* sp.	Dominica	JQ948195	JQ948525	JQ948856	JQ949186	JQ949516	JQ949846
C. eriobotryae	**GLMC 1935**	Acutatum	*Eriobotrya japonica*	China	MF772487	MF795423	MN191653	MN191658	MN191648	MF795428
C. fioriniae	**CBS 128517**	Acutatum	*Fiorinia externa*	USA	JQ948292	JQ948622	JQ948953	JQ949283	JQ949613	JQ949943
C. godetiae	**CBS 133.44**	Acutatum	*Clarkia hybrida* cv. *Kelvon Glory*	Denmark	JQ948402	JQ948733	JQ949063	JQ949393	JQ949723	JQ950053
	NFUCo-1 [c]	Acutatum	*Cy. paliurus*	Guizhou, China	*OR064051*	*OR069507*	*OR073858*	*OR096497*	*OR096424*	*OR096472*
	NFUCo-4 [c]	Acutatum	*Cy. paliurus*	Jiangxi, China	*OR064052*	*OR069508*	*OR073859*	*OR096498*	*OR096425*	*OR096473*
	NFUCo-5 [c]	Acutatum	*Cy. paliurus*	Hunan, China	*OR064053*	*OR069509*	*OR073860*	*OR096499*	*OR096426*	*OR096474*
	NFUCo-8	Acutatum	*Cy. paliurus*	Hunan, China	*OR064054*	*OR069510*	*OR073861*	*OR096500*	*OR096427*	*OR096475*

Table A2. *Cont.*

Species	Culture/ Isolate [a]	Clade	Host	Location	GenBank Accession Number [b]					
					ITS	*GAPDH*	*CHS-1*	*HIS3*	*ACT*	*TUB2*
	NFUCo-11	Acutatum	*Cy. paliurus*	Hunan, China	*OR064055*	*OR069511*	*OR073862*	*OR096501*	*OR096428*	*OR096476*
C. guajavae	**IMI 350839**	Acutatum	*Psidium guajava*	India	JQ948270	JQ948600	JQ948931	JQ949261	JQ949591	JQ949921
C. indonesiense	**CBS 127551**	Acutatum	*Eucalyptus* sp.	Indonesia	JQ948288	JQ948618	JQ948949	JQ949279	JQ949609	JQ949939
C. javanense	**CBS 144963**	Acutatum	*Capsicum annuum*	Indonesia	MH846576	MH846572	MH846573	MH846571	MH846575	MH846574
C. johnstonii	**CBS 128532**	Acutatum	*Solanum lycopersicum*	New Zealand	JQ948444	JQ948775	JQ949105	JQ949435	JQ949765	JQ950095
C. kinghornii	**CBS 198.35**	Acutatum	*Phormium* sp.	UK	JQ948454	JQ948785	JQ949115	JQ949445	JQ949775	JQ950105
C. laticiphilum	**CBS 112989**	Acutatum	*Hevea brasiliensis*	India	JQ948289	JQ948619	JQ948950	JQ949280	JQ949610	JQ949940
C. limetticola	**CBS 114.14**	Acutatum	*Citrus aurantifolia*	USA, Florida	JQ948193	JQ948523	JQ948854	JQ949184	JQ949514	JQ949844
C. lobatum	**IMI 79736**	Magnum	*Piper catalpaefolium*	Trinidad	MG600768	MG600828	MG600874	MG600912	MG600972	MG601035
C. lupini	**CBS 109225**	Acutatum	*Lupinus albus*	Ukraine	JQ948155	JQ948485	JQ948816	JQ949146	JQ949476	JQ949806
C. magnum	**CBS 519.97**	Magnum	*Citrullus lanatus*	USA	MG600769	MG600829	MG600875	MG600913	MG600973	MG601036
C. melonis	**CBS 159.84**	Acutatum	*Cucumis melo*	Brazil	JQ948194	JQ948524	JQ948855	JQ949185	JQ949515	JQ949845
C. merremiae	**CBS 124955**	Magnum	*Merremia umbellata*	Panama	MG600765	MG600825	MG600872	MG600910	MG600969	MG601032
C. monsterae	**LC13871**	Orchidearum	Monstera deliciosa	China	MZ595897	MZ664121	MZ799351	MZ673917	MZ664195	MZ674015
C. musicola	**CBS 132885**	Orchidearum	*Musa* sp.	Mexico	MG600736	MG600798	MG600853	MG600895	MG600942	MG601003
C. nymphaeae	**CBS 515.78**	Acutatum	*Nymphaea alba*	Netherlands	JQ948197	JQ948527	JQ948858	JQ949188	JQ949518	JQ949848
	NFUCN-2 [c]	Acutatum	*Cy. paliurus*	Guangxi, China	*OR064071*	*OR069527*	*OR073878*	*OR096517*	*OR096444*	*OR096492*
	NFUCN-5 [c]	Acutatum	*Cy. paliurus*	Hunan, China	*OR064072*	*OR069528*	*OR073879*	*OR096518*	*OR096445*	*OR096493*
	NFUCN-7	Acutatum	*Cy. paliurus*	Hunan, China	*OR064073*	*OR069529*	*OR073880*	*OR096519*	*OR096446*	*OR096494*
	NFUCN-11 [c]	Acutatum	*Cy. paliurus*	Guizhou, China	*OR064074*	*OR069530*	*OR073881*	*OR096520*	*OR096447*	*OR096495*
	NFUCN-14	Acutatum	*Cy. paliurus*	Jiangxi, China	*OR064075*	*OR069531*	*OR073882*	*OR096521*	*OR096448*	*OR096496*
C. orchidearum	**CBS 135131**	Orchidearum	*Dendrobium nobile*	Netherlands	MG600738	MG600800	MG600855	MG600897	MG600944	MG601005
C. panamense	**CBS 125386**	Magnum	*Merremia umbellata*	Panama	MG600766	MG600826	MG600873	MG600911	MG600970	MG601033
C. paxtonii	**IMI 165753**	Acutatum	*Musa* sp.	Saint Lucia	JQ948285	JQ948615	JQ948946	JQ949276	JQ949606	JQ949936
C. phormii	**CBS 118194**	Acutatum	*Phormium* sp.	Germany	JQ948446	JQ948777	JQ949107	JQ949437	JQ949767	JQ950097
C. piperis	**IMI 71397**	Orchidearum	*Piper nigrum*	Malaysia	MG600760	MG600820	MG600867	MG600906	MG600964	MG601027
C. plurivorum	**CBS 125474**	Orchidearum	*Coffea* sp.	Vietnam	MG600718	MG600781	MG600841	MG600887	MG600925	MG600985
	NFUCP-3 [c]	Orchidearum	*Cy. paliurus*	Guizhou, China	*OR064066*	*OR069522*	*OR073873*	*OR096512*	*OR096439*	*OR096487*
	NFUCP-5 [c]	Orchidearum	*Cy. paliurus*	Hunan, China	*OR064067*	*OR069523*	*OR073874*	*OR096513*	*OR096440*	*OR096488*
	NFUCP-7	Orchidearum	*Cy. paliurus*	Hunan, China	*OR064068*	*OR069524*	*OR073875*	*OR096514*	*OR096441*	*OR096489*
	NFUCP-8	Orchidearum	*Cy. paliurus*	Hunan, China	*OR064069*	*OR069525*	*OR073876*	*OR096515*	*OR096442*	*OR096490*
	NFUCP-13 [c]	Orchidearum	*Cy. paliurus*	Jiangxi, China	*OR064070*	*OR069526*	*OR073877*	*OR096516*	*OR096443*	*OR096491*
C. pyricola	**CBS 128531**	Acutatum	*Pyrus communis*	New Zealand	JQ948445	JQ948776	JQ949106	JQ949436	JQ949766	JQ950096
C. reniforme	**LC8230**	Orchidearum	*Smilax cocculoides*	China	MZ595847	MZ664110	MZ799290	MZ673867	MZ664145	MZ673968
C. rhombiforme	**CBS 129953**	Acutatum	*Olea europaea*	Portugal	JQ948457	JQ948788	JQ949118	JQ949448	JQ949778	JQ950108
C. salicis	**CBS 607.94**	Acutatum	*Salix* sp.	Netherlands	JQ948460	JQ948791	JQ949121	JQ949451	JQ949781	JQ950111
C. schimae	**LC13880**	Acutatum	Schima sp.	China	MZ595885	MZ664105	MZ799347	MZ673905	MZ664183	MZ674003
C. scovillei	**CBS 126529**	Acutatum	*Capsicum* sp.	Indonesia	JQ948267	JQ948597	JQ948928	JQ949258	JQ949588	JQ949918
C. simmondsii	**CBS 122122**	Acutatum	*Carica papaya*	Australia	JQ948276	JQ948606	JQ948937	JQ949267	JQ949597	JQ949927
C. sloanei	**IMI 364297**	Acutatum	*Theobroma cacao*	Malaysia	JQ948287	JQ948617	JQ948948	JQ949278	JQ949608	JQ949938
C. sojae	**ATCC 62257**	Orchidearum	*Glycine max*	USA	MG600749	MG600810	MG600860	MG600899	MG600954	MG601016
	NFUCS-1 [c]	Orchidearum	*Cy. paliurus*	Jiangxi, China	*OR064056*	*OR069512*	*OR073863*	*OR096502*	*OR096429*	*OR096477*
	NFUCS-3 [c]	Orchidearum	*Cy. paliurus*	Hunan, China	*OR064057*	*OR069513*	*OR073864*	*OR096503*	*OR096430*	*OR096478*
	NFUCS-6	Orchidearum	*Cy. paliurus*	Hunan, China	*OR064058*	*OR069514*	*OR073865*	*OR096504*	*OR096431*	*OR096479*

Table A2. *Cont.*

Species	Culture/ Isolate [a]	Clade	Host	Location	GenBank Accession Number [b]					
					ITS	*GAPDH*	*CHS-1*	*HIS3*	*ACT*	*TUB2*
	NFUCS-10 [c]	Orchidearum	*Cy. paliurus*	Guizhou, China	*OR064059*	*OR069515*	*OR073866*	*OR096505*	*OR096432*	*OR096480*
	NFUCS-15	Orchidearum	*Cy. paliurus*	Fujian, China	*OR064060*	*OR069516*	*OR073867*	*OR096506*	*OR096433*	*OR096481*
C. tamarilloi	**CBS 129814**	Acutatum	*Solanum betaceum*	Colombia	JQ948184	JQ948514	JQ948845	JQ949175	JQ949505	JQ949835
C. vittalense	**CBS 181.82**	Orchidearum	*Theobroma cacao*	India	MG600734	MG600796	MG600851	MG600893	MG600940	MG601001
C. walleri	**CBS 125472**	Acutatum	*Coffea* sp.	Vietnam	JQ948275	JQ948605	JQ948936	JQ949266	JQ949596	JQ949926
Monilochaetes infuscans	CBS 869.96	outgroup	*Ipomoea batatas*	South Africa	JQ005780	JX546612	JQ005801	JQ005822	JQ005843	JQ005864

[a] Culture numbers in bold type represent ex-type or other authentic specimens. CBS 869.96 (*Monilochaetes infuscans*) was added as an outgroup. [b] Sequences in italics were generated in this study. [c] Isolates used for phenotypic analysis and virulence tests.

Table A3. Location information and incidence rate statistics of the investigated area.

Province	County/Location	Leaf Samples	Latitude (N)	Longitude (E)
Fujian	Xiapu	4	27°03′08″	119°56′33″
	Jianyang	6	27°33′08″	117°47′03″
Guangxi	Longsheng	7	26°01′13″	109°55′08″
Guizhou	Lipin	12	26°06′50″	109°11′08″
Hubei	Yidu	6	30°26′04″	111°19′54″
	Sui	6	32°11′43″	113°16′11″
Hunan	Jianghua Yao nationality	13	24°54′01″	112°06′43″
Jiangxi	Jinggangshan	6	26°42′03″	114°17′47″
	Shangrao	7	28°49′54″	118°11′07″
Sichuan	Xuyong	5	28°09′11″	105°23′54″
Zhejiang	Lanxi	11	29°08′50″	119°23′28″

References

1. Zhao, W.; Tang, D.; Yuan, E.; Wang, M.; Zhang, Q.; Liu, Y.; Shen, B.; Chen, J.; Yin, Z. Inducement and cultivation of novel red *Cyclocarya paliurus* callus and its unique morphological and metabolic characteristics. *Ind. Crops Prod.* **2020**, *147*, 30–33. [CrossRef]
2. Yang, Z.; Wang, J.; Li, J.; Xiong, L.; Chen, H.; Liu, X.; Wang, N.; Ouyang, K.; Wang, W. Antihyperlipidemic and hepatoprotective activities of polysaccharide fraction from *Cyclocarya paliurus* in high-fat emulsion-induced hyperlipidaemic mice. *Carbohydr. Polym.* **2018**, *183*, 11–20. [CrossRef] [PubMed]
3. Li, Q.; Hu, J.; Nie, Q.; Chang, X.; Fang, Q.; Xie, J.; Li, H.; Nie, S.P. Hypoglycemic mechanism of polysaccharide from *Cyclocarya paliurus* leaves in type 2 diabetic rats by gut microbiota and host metabolism alteration. *Sci. China Life Sci.* **2020**, *64*, 117–132. [CrossRef] [PubMed]
4. Shen, Y.; Peng, Y.; Zhu, X.; Li, H.; Zhang, L.; Kong, F.; Wang, J.; Yu, D. The phytochemicals and health benefits of *Cyclocarya paliurus* (Batalin) Iljinskaja. *Front. Nutr.* **2023**, *10*, 1158158. [CrossRef] [PubMed]
5. Lei, X.; Hu, W.B.; Yang, Z.W.; Chen, H.; Wang, N.; Liu, X.; Wang, W. Enzymolysis-ultrasonic assisted extraction of flavanoid from *Cyclocarya paliurus* (Batal) Iljinskaja: HPLC profile, antimicrobial and antioxidant activity. *Ind. Crops Prod.* **2019**, *130*, 615–626.
6. Tu, W.C.; Luo, H.R.; Yuan, E.; Sakah, J.; Yang, Q.Y.; Xiao, W.L.; Zheng, Y.T.; Liu, M.F. Triterpene constituents from the fruits of *Cyclocarya paliurus* and their anti-HIV-1 IIIB activity. *Nat. Prod. Res.* **2022**, *37*, 1787–1796. [CrossRef] [PubMed]
7. Zhou, M.; Quek, S.Y.; Shang, X.; Fang, S. Geographical variations of triterpenoid contents in *Cyclocarya paliurus* leaves and their inhibitory effects on HeLa cells. *Ind. Crops Prod.* **2021**, *162*, 113314. [CrossRef]
8. Li, X.; Fu, X.; Shang, X.; Yang, W.; Fang, S. Natural population structure and genetic differentiation for heterodicogamous plant: *Cyclocarya paliurus* (Batal.) Iljinskaja (Juglandaceae). *Tree Genet. Genomes* **2017**, *13*, 80. [CrossRef]
9. Zheng, X.R.; Liu, C.L.; Zhang, M.J.; Shang, X.L.; Fang, S.Z.; Chen, F.M. First report of leaf blight of *Cyclocarya paliurus* caused by *Nigrospora sphaerica* in China. *Crop Prot.* **2020**, *140*, 105453. [CrossRef]
10. Zheng, X.R.; Zhang, M.J.; Shang, X.L.; Fang, S.Z.; Chen, F.M. Etiology of *Cyclocarya paliurus* Anthracnose in Jiangsu Province, China. *Front. Plant Sci.* **2021**, *11*, 613499. [CrossRef]
11. Wang, Y.; Chen, J.; Xu, X.; Cheng, J.; Zheng, L.; Huang, J.; Li, D.W. Identification and Characterization of *Colletotrichum* Species Associated with Anthracnose Disease of *Camellia oleifera* in China. *Plant Dis.* **2020**, *104*, 474–482. [CrossRef] [PubMed]
12. Hyde, K.; Cai, L.; Cannon, P.; Crouch, J.A.; Crous, P.; Damm, U.; Goodwin, P.H.; Chen, H.; Johnston, P.; Jones, E.; et al. *Colletotrichum*—Names in current use. *Fungal Divers.* **2009**, *39*, 147–182.
13. Weir, B.S.; Johnston, P.R.; Damm, U. The *Colletotrichum gloeosporioides* species complex. *Stud. Mycol.* **2012**, *73*, 115–180. [CrossRef]

14. Liu, F.; Ma, Z.Y.; Hou, L.; Diao, Y.; Wu, W.; Damm, U.; Song, S.; Cai, L. Updating species diversity of *Colletotrichum*, with a phylogenomic overview. *Stud. Mycol.* **2022**, *101*, 1–56. [CrossRef]
15. Damm, U.; Sato, T.; Alizadeh, A.; Groenewald, J.Z.; Crous, P.W. The *Colletotrichum dracaenophilum*, *C. magnum* and *C. orchidearum* species complexes. *Stud. Mycol.* **2019**, *92*, 1–46. [CrossRef] [PubMed]
16. Damm, U.; Cannon, P.F.; Woudenberg, J.H.C.; Crous, P.W. The *Colletotrichum acutatum* species complex. *Stud. Mycol.* **2012**, *73*, 37–113. [CrossRef] [PubMed]
17. Liu, F.; Weir, B.; Damm, U.; Crous, P.; Wang, Y.; Liu, B.; Wang, M.; Zhang, M.; Cai, L. Unravelling *Colletotrichum* species associated with *Camellia*: Employing *ApMat* and *GS* loci to resolve species in the *C. gloeosporioides* complex. *Persoonia* **2016**, *35*, 63–86. [CrossRef] [PubMed]
18. Fu, M.; Crous, P.W.; Bai, Q.; Zhang, P.F.; Xiang, J.; Guo, Y.S.; Zhao, F.F.; Yang, M.M.; Hong, N.; Xu, W.X.; et al. *Colletotrichum* species associated with anthracnose of *Pyrus* spp. in China. *Persoonia* **2019**, *42*, 1–35. [CrossRef]
19. Cai, L.; Hyde, K.; Taylor, P.; Weir, B.; Waller, J.; Abang, M.; Zhang, J.Z.; Yang, Y.L.; Phoulivong, S.; Liu, Z.Y. A polyphasic approach for studying *Colletotrichum*. *Fungal Divers.* **2009**, *39*, 183–204.
20. Gardes, M.; Bruns, T. ITS primers with enhanced specificity for basidiomycetes—Application to the identification of mycorrhizae and rusts. *Mol. Ecol.* **1993**, *2*, 113–118. [CrossRef]
21. White, T.; Bruns, T.; Lee, S.; Taylor, J.; Innis, M.; Gelfand, D.; Sninsky, J. Amplification and direct sequencing of fungal ribosomal RNA genes for phylogenetics. In *PCR Protocols: A Guide to Methods and Applications*; Academic Press: Cambridge, MA, USA, 1990; pp. 315–322.
22. Guerber, J.C.; Liu, B.; Correll, J.C.; Johnston, P.R. Characterization of diversity in *Colletotrichum acutatum* sensu lato by sequence analysis of two gene introns, mtDNA and intron RFLPs, and mating compatibility. *Mycologia* **2003**, *95*, 872–895. [CrossRef] [PubMed]
23. Carbone, I.; Kohn, L.M. A method for designing primer sets for speciation studies in filamentous ascomycetes. *Mycologia* **1999**, *91*, 553–556. [CrossRef]
24. Crous, P.W.; Groenewald, J.Z.; Risede, J.M.; Simoneau, P.; Hywel-Jones, N.L. Calonectria species and their *Cylindrocladium anamorphs*: Species with sphaeropedunculate vesicles. *Stud. Mycol.* **2004**, *50*, 415–430.
25. O'Donnell, K.; Cigelnik, E. Two divergent intragenomic rDNA ITS2 types within a monophyletic lineage of the fungus *Fusarium* are nonorthologous. *Mol. Phylogenet. Evol.* **1997**, *7*, 103–116. [CrossRef]
26. Glass, N.L.; Donaldson, G.C. Development of primer sets designed for use with the PCR to amplify conserved genes from filamentous ascomycetes. *Appl. Environ. Microbiol.* **1995**, *61*, 1323–1330. [CrossRef]
27. O'Donnell, K.; Nirenberg, H.I.; Aoki, T.; Cigelnik, E. A Multigene phylogeny of the *Gibberella fujikuroi* species complex: Detection of additional phylogenetically distinct species. *Mycoscience* **2000**, *41*, 61–78. [CrossRef]
28. Silva, D.N.; Talhinhas, P.; Varzea, V.; Cai, L.; Paulo, O.S.; Batista, D. Application of the Apn2/MAT locus to improve the systematics of the *Colletotrichum gloeosporioides* complex: An example from coffee (Coffea spp.) hosts. *Mycologia* **2012**, *104*, 396–409. [CrossRef]
29. Vaidya, G.; Lohman, D.J.; Meier, R. SequenceMatrix: Concatenation software for the fast assembly of multi-gene datasets with character set and codon information. *Cladistics* **2011**, *27*, 171–180. [CrossRef]
30. Kumar, S.; Stecher, G.; Li, M.; Knyaz, C.; Tamura, K. MEGA X: Molecular Evolutionary Genetics Analysis across Computing Platforms. *Mol. Biol. Evol.* **2018**, *35*, 1547–1549. [CrossRef]
31. Ronquist, F.; Teslenko, M.; Mark, P.; Ayres, D.; Darling, A.; Höhna, S.; Larget, B.; Liu, L.; Suchard, M.; Huelsenbeck, J. MrBayes 3.2: Efficient Bayesian Phylogenetic Inference and Model Choice Across a Large Model Space. *Syst. Biol.* **2012**, *61*, 539–542. [CrossRef]
32. Zheng, X.R.; Zhang, M.J.; Qiao, Y.H.; Li, R.; Alkan, N.; Chen, J.Y.; Chen, F.M. *Cyclocarya paliurus* Reprograms the Flavonoid Biosynthesis Pathway Against *Colletotrichum fructicola*. *Front. Plant Sci.* **2022**, *13*, 933484. [CrossRef] [PubMed]
33. He, L.F.; Li, X.X.; Gao, Y.Y.; Li, B.X.; Mu, W.; Liu, F. Characterization and Fungicide Sensitivity of *Colletotrichum* spp. from Different Hosts in Shandong, China. *Plant Dis.* **2019**, *103*, 34–43. [CrossRef] [PubMed]
34. Freeman, S.; Katan, T.; Shabi, E. Characterization of *Colletotrichum* Species Responsible for Anthracnose Diseases of Various Fruits. *Plant Dis.* **1998**, *82*, 596–605. [CrossRef] [PubMed]
35. Freeman, S.; Horowitz, S.; Sharon, A. Pathogenic and Nonpathogenic Lifestyles in *Colletotrichum acutatum* from Strawberry and other Plants. *Phytopathology* **2001**, *91*, 986–992. [CrossRef] [PubMed]
36. Schoch, C.; Seifert, K.; Huhndorf, S.M.; Robert, V.; Spouge, J.; Levesque, C.; Chen, W.; Janzen, D.; Consortium, A. Nuclear ribosomal internal transcribed spacer (ITS) region as a universal DNA barcode marker for Fungi. *Proc. Natl. Acad. Sci. USA* **2012**, *109*, 6241–6246. [CrossRef] [PubMed]
37. Hyde, K.D.; Nilsson, R.H.; Alias, S.A.; Ariyawansa, H.A.; Blair, J.E.; Cai, L.; Cock, A.W.A.M.; Dissanayake, A.J.; Glockling, S.L.; Goonasekara, I.D.; et al. One stop shop: Backbones trees for important phytopathogenic genera: I. *Fungal Divers.* **2014**, *67*, 21–125. [CrossRef]
38. Tovar-Pedraza, J.M.; Mora-Aguilera, J.A.; Nava-Díaz, C.; Lima, N.B.; Michereff, S.J.; Sandoval-Islas, J.S.; Câmara, M.P.S.; Téliz-Ortiz, D.; Leyva-Mir, S.G. Distribution and Pathogenicity of *Colletotrichum* Species Associated with Mango Anthracnose in Mexico. *Plant Dis.* **2020**, *104*, 137–146. [CrossRef]
39. Prihastuti, H.; McKenzie, E.; Hyde, K.; Cai, L.; Hu, M.; Hyde, E. Characterization of *Colletotrichum* species associated with coffee berries in northern Thailand. *Fungal Divers.* **2009**, *39*, 89–109.

40. Wang, W.; de Silva, D.D.; Moslemi, A.; Edwards, J.; Ades, P.K.; Crous, P.W.; Taylor, P.W.J. *Colletotrichum* Species Causing Anthracnose of Citrus in Australia. *J. Fungi* **2021**, *7*, 47. [CrossRef]
41. Eaton, M.; Edwards, S.; Inocencio, H.; Machado, F.; Nuckles, E.; Farman, M.; Gauthier, N.; Vaillancourt, L. Diversity and Cross-Infection Potential of *Colletotrichum* Causing Fruit Rots in Mixed-Fruit Orchards in Kentucky. *Plant Dis.* **2020**, *105*, 1115–1128. [CrossRef]
42. Moreira, R.R.; Peres, N.A.; May, D.M.L.L. *Colletotrichum acutatum* and *C. gloeosporioides* Species Complexes Associated with Apple in Brazil. *Plant Dis.* **2019**, *103*, 268–275. [CrossRef] [PubMed]
43. Noor, N.M.; Zakaria, L. Identification and characterization of *Colletotrichum* spp. associated with chili anthracnose in peninsular Malaysia. *Eur. J. Plant Pathol.* **2018**, *151*, 961–973. [CrossRef]
44. Zhang, L.; Li, X.; Zhou, Y.; Tan, G.; Zhang, L. Identification and characterization of *Colletotrichum* species associated with *Camellia sinensis* anthracnose in Anhui province, China. *Plant Dis.* **2020**, *105*, 2649–2657. [CrossRef]
45. Jian, Y.; Li, Y.; Tang, G.; Zheng, X.; Khaskheli, M.I.; Gong, G. Identification of *Colletotrichum* Species Associated with Anthracnose Disease of Strawberry in Sichuan Province, China. *Plant Dis.* **2021**, *105*, 3025–3036. [CrossRef] [PubMed]
46. Chen, Y.; Fu, D.; Wang, W.; Gleason, M.L.; Zhang, R.; Liang, X.; Sun, G. Diversity of *Colletotrichum* Species Causing Apple Bitter Rot and Glomerella Leaf Spot in China. *J. Fungi* **2022**, *8*, 740. [CrossRef] [PubMed]
47. Tan, Q.; Schnabel, G.; Chaisiri, C.; Yin, L.; Yin, W.; Luo, C. *Colletotrichum* Species Associated with Peaches in China. *J. Fungi* **2022**, *8*, 313. [CrossRef] [PubMed]
48. Mo, J.; Zhao, G.; Li, Q.; Solangi, G.S.; Tang, L.; Guo, T.; Huang, S.; Hsiang, T. Identification and Characterization of *Colletotrichum* Species Associated with Mango Anthracnose in Guangxi, China. *Plant Dis.* **2018**, *102*, 1283–1289. [CrossRef] [PubMed]
49. Wan, Y.; Jin, G.; Li, D.; Wu, S.; Zhu, L. First report of *Colletotrichum fructicola* causing leaf spots on *Liriodendron chinense* × *tulipifera* in China. *Forest Pathol.* **2022**, *52*, e12779. [CrossRef]